

## **ABSTRACT**

Title of Thesis: AN EXPLICATION OF AIRFOIL SECTION BENDING-TORSION FLUTTER

Philip Curtis Wheeler, Master of Science, 2004

Thesis directed by: Professor Ricardo Medina

Department of Civil and Environmental Engineering

This thesis examines the dynamic instability known as flutter using a two-degree-of-freedom airfoil section model in both quasi-steady and unsteady flow. It explains the fundamental forces and moments involved in the bending-torsion flutter of an airfoil section, and demonstrates a solution method for determining the critical flutter frequency and speed for

both flow cases. Additionally, through the use of a programmed Mathcad 11 worksheet, it evaluates the flutter characteristics of six example sections, illustrating the effects of the elastic, inertial and aerodynamic properties of an airfoil section. For each section, a parametric study of the effect of the section Center of Gravity position along the section chord is performed. The flutter frequency and speed are calculated using both quasi-steady and unsteady aerodynamic forces and moments, and the results compared. Software used was MathSoft Mathcad 11, Microsoft Word and Intergraph Smart Sketch LE.

**AN EXPLICATION OF AIRFOIL SECTION BENDING-TORSION  
FLUTTER**

by

Philip Curtis Wheeler

Thesis submitted to the Faculty of the Graduate School of the  
University of Maryland, College Park in partial fulfillment  
of the requirements for the degree of  
Master of Science  
2004

Advisory Committee:

Professor Ricardo Medina, Chair  
Professor Pedro Albrecht  
Professor Bruce K. Donaldson

©Copyright by  
Philip Curtis Wheeler  
2004

## **Acknowledgements**

The author wishes to thank Dr. Bruce Donaldson for his assistance in preparing this scholarly paper.

The author also wishes to thank Dr. Ricardo Medina and Dr. Pedro Albrecht for their review of this paper.

This Page Intentionally Left Blank

## Table of Contents

List of Tables.....	x
List of Figures.....	xi
List of Symbols and Abbreviations .....	xii
Chapter 1.0: Introduction.....	1
1.1 Motivation for the thesis.....	1
1.2 Objectives of the thesis .....	2
1.3 Thesis Organization.....	3
1.4 Chapter Summary .....	3
Chapter 2.0: A Fundamental Description of Flutter .....	5
2.1 Types of Aeroelasticity .....	5
2.2 Distinctive Characteristics of Classical Airfoil Section Flutter .....	8
2.3 Types of Airfoil Section Flutter .....	10
2.3.1 Vibratory modes.....	11
2.3.2 Examples of Airfoil Section Flutter with Increasing Numbers of Types of Motion .....	11
2.4 Bending-torsion Flutter of an Airfoil Section as Described in this Thesis .....	12
2.4.1 Defining the Degrees of Freedom.....	14
2.5 Chapter Summary .....	15

Chapter 3.0: Solutions for the Flutter Frequency and Speed .....	17
3.1 Derivation of the Lagrange Equations of Motion.....	17
3.1.1 Strain Energy of Elastic Forces.....	19
3.1.2 Kinetic Energy of Inertial Forces .....	19
3.1.3 Generalized Forces .....	20
3.2 Writing the Lagrange Equations of Motion.....	21
3.3 Energy Transfer and Coupling.....	24
3.3.1 Energy Transfer from the Airstream.....	24
3.3.2 Inertial coupling due to Center of Gravity location .....	25
3.3.3 Phasing of the Motions .....	26
3.3.4 Aerodynamic Coupling via Phasing .....	26
3.4 Frequency Coalescence .....	28
3.5 Phasing Diagrams .....	29
3.5.1 Stable Condition .....	29
3.5.2 Critical Flutter Condition.....	30
3.5.3 Full Flutter Condition.....	31
3.6 Aerodynamic Forces.....	32
3.6.1 Fluid Properties.....	33
3.6.2 Basic strip theory .....	35
3.6.3 Two Dimensional Airfoil Section Properties .....	36
3.6.4 Development of the Quasi-steady Aerodynamic Forces.....	37
3.6.4.1 Aerodynamic Moment .....	38
3.6.4.2 Forming the Lagrange Equations of Motion using Quasi-steady Aerodynamic Forces .....	40
3.6.5 Development of the Unsteady Aerodynamic Forces.....	42

3.6.5.1 Forming the Lagrange Equations of Motion using Unsteady Aerodynamic Forces and Moments .....	43
3.6.5.1.1 Finding the flutter frequency and speed – Theodorsen’s Method .....	44
3.6.5.1.2 Finding the flutter frequency and speed – Materiel Center Method .....	45
3.7 Solution of the Double Eigenvalue Problem .....	46
3.7.1 Placing the System in Simple Harmonic Motion.....	47
3.7.1.1 Flutter Solution in the case of Quasi-steady Aerodynamic Forces .....	49
3.7.1.2 Flutter Solution in the Case of Unsteady Aerodynamic Forces and Moments ..	51
3.8 Chapter Summary .....	61
Chapter 4.0: Calculation of Flutter Properties by Mathcad Worksheet .....	63
4.1 Mathcad Worksheet Methodology .....	63
4.1.1 Program inputs .....	64
4.1.2 Supporting calculations.....	65
4.1.2.1 Quasi-steady Case.....	65
4.1.2.2 Unsteady Case.....	65
4.1.3 Primary calculations.....	67
4.1.3.1 Quasi-steady Case.....	67
4.1.3.2 Unsteady Case.....	67
4.1.4 Program Outputs .....	68
4.2 Example Calculations . .....	69
4.2.1 Example One: Ryan NYP prototype	

(Blevins, 1990).....	70
4.2.1.1 Inputs, Intermediate Calculations and Output .....	70
4.2.1.2 Section Characteristics .....	71
4.2.1.3. Flutter Calculations for the Quasi-steady Case.....	72
4.2.1.4 Flutter Calculations for the Unsteady Case .....	72
4.2.1.5 Comparison of Results in the Quasi- steady and Unsteady Cases .....	73
4.2.1.6 CG Variation Survey .....	73
4.2.2 Example Two: Ryan NYP Final Design (Blevins, 1990).....	75
4.2.2.1 Inputs, Intermediate Calculations and Outputs .....	75
4.2.2.2 Section Characteristics .....	76
4.2.2.3. Flutter Calculations for the Quasi-steady Case.....	76
4.2.2.4 Flutter Calculations for the Unsteady Case .....	77
4.2.2.5 Comparison of Results in the Quasi- steady and Unsteady Cases .....	78
4.2.2.6 CG Variation Survey .....	78
4.2.3 Example Three: MD3-160 Aircraft Section (Usmani, Ho, 2003). .....	79
4.2.3.1 Inputs, Intermediate Calculations and Outputs .....	79
4.2.3.2 Section Characteristics .....	80
4.2.3.3. Flutter Calculations for the Quasi-steady Case.....	81
4.2.3.4 Flutter Calculations for the Unsteady Case .....	81
4.2.3.5 Comparison of Results in the Quasi- steady and Unsteady Cases .....	82
4.2.3.6 Altitude Variation Survey .....	82
4.2.2.7 CG Variation Survey .....	84

4.2.4 Example Four: Example from NACA Technical Report 685, (Theodorsen, Garrick, 1938).....	85
4.2.4.1 Inputs, Intermediate Calculations and Outputs .....	85
4.2.4.2 Section Characteristics .....	86
4.2.4.3. Flutter Calculations for the Quasi-steady Case.....	87
4.2.4.4 Flutter Calculations for the Unsteady Case .....	87
4.2.4.5 Comparison of Results in the Quasi-steady and Unsteady Cases .....	87
4.2.4.6 CG Variation Survey .....	88
4.2.5 Example Five: Example from USAAF Technical Report 4798, (Smilg, Wasserman, 1942).....	89
4.2.5.1 Inputs, Intermediate Calculations and Outputs .....	89
4.2.5.2 Section Characteristics .....	90
4.2.5.3. Flutter Calculations for the Quasi-steady Case.....	91
4.2.5.4 Flutter Calculations for the Unsteady Case .....	91
4.2.5.5 Comparison of Results in the Quasi-steady and Unsteady Cases .....	91
4.2.5.6 CG Variation Survey .....	92
4.2.6 Example Six: Example from Reference 5, page 203 (Scanlan, Rosenbaum, 1968) .....	93
4.2.6.1 Inputs, Intermediate Calculations and Outputs .....	93
4.2.6.2 Section Characteristics .....	94
4.2.6.3. Flutter Calculations for the Quasi-steady Case.....	94
4.2.6.4 Flutter Calculations for the Unsteady Case .....	95
4.2.6.5 Comparison of Results in the Quasi-steady and Unsteady Cases .....	95
4.2.6.6 CG Variation Survey .....	95
4.3 Chapter Summary .....	97

Appendix .....	103
References .....	125

## List of Tables

Table 3.6.3: Airfoil Section Data .....	36
Table 4.2.3.7: Flutter Speed Variation with Altitude .....	83
Table 4.3: Summary of Program Inputs, Calculations and Outputs..	99

## List of Figures

Figure 2.1: Summary of Forces and Responses .....	6
Figure 2.4: Two DOF Model.....	14
Figure 3.3.2: Inertial Coupling as a Function of CG Position.....	26
Figure 3.5.1: Stable Vertical and Torsional Oscillations .....	30
Figure 3.5.2: Critical Flutter (Stability Boundary) Condition.....	31
Figure 3.5.3: Full Flutter Condition .....	32
Figure 3.6.2: Basic Strip Theory .....	35
Figure 3.6.3: Lift Curve and Aerodynamic Moment Slopes .....	40
Figure 3.7.1.2.1: Artificial Damping versus Reduced Frequency.....	60
Figure 3.7.1.2.2: Artificial Damping versus Velocity .....	61
Figure 4.2.3.7: Graph of Flutter Speed Variation with Altitude .....	83

## List of Symbols and Abbreviations

Symbol	Definition	Unit
a	Distance from section elastic axis to section aerodynamic center, positive forward of elastic axis.	in
a <sub>h</sub>	Location of section elastic axis from section midchord, positive aft of midchord.	Non-Dimensional
b	Distance from section elastic axis to section center of gravity, positive forward of elastic axis, equal to $(a_h - x_{\alpha}) \cdot b'$	in
b'	Section semi-chord, equal to c/2.	in
c	Section chord; distance from the leading edge to trailing edge, positive aft of leading edge.	in
deg	Degrees	
f <sub>b</sub>	Uncoupled bending frequency	Hz
f <sub>fl</sub>	Coupled flutter frequency using unsteady aerodynamics	Hz
f <sub>Qs</sub>	Coupled flutter frequency using quasi-steady aerodynamics	Hz
f <sub>T</sub>	Uncoupled torsional frequency	Hz
g	Artificial damping coefficient, a variable used in the solution of the flutter stability determinant.	Non- Dimensional

h	Vertical translation of section; first degree of freedom of section, measured for the Quasi-steady case positive up from the elastic axis, and for the Unsteady case positive down.	in
$\frac{h}{b'}$	Non - Dimensionalized vertical translation of section	Non- Dimensional
i	$\sqrt{-1}$	
k	Reduced frequency, the ratio between the section oscillation frequency and the fictitious frequency equal to the number of times per second the section, due to its forward speed, traverses a distance equal to its semi-schord; equal to $\frac{\omega_{fl} \cdot b'}{V_{fl}}$ .	Non- Dimensional
$k_b$	Section bending stiffness per unit span	$\frac{\text{in} \cdot \text{lbf}}{\text{in}}$
knots	Nautical miles per hour	
lbf	Pound force	pounds
m	Section mass per unit span slug	
q	Dynamic pressure	$\frac{\text{lbf}}{\text{in}^2}$
qD	Static divergence dynamic pressure	$\frac{\text{lbf}}{\text{in}^2}$
$r_\alpha$	Dimensionless section radius of gyration per unit span about the EA, equal to $\sqrt{\frac{H_{ea}}{m \cdot b'^2}}$	Non- Dimensional

rad	Radians	
t	Time	seconds
w	Section span	in
w.r.t.	Abbreviation for "with respect to"	
$x_{\alpha}$	Location of section CG, positive aft of EA.	Non- Dimensional
A	Bending flutter determinant element for h/b'	Non- Dimensional
$A_0$	Aerodynamic lift factor , equal to $\frac{1}{2} \cdot \rho \cdot S \cdot C_{l\alpha}$	$\frac{\text{slug} \cdot \text{in}}{\text{rad}}$
AC	Location of section aerodynamic center; the point along the section chord where all changes in lift take place and where the aerodynamic moment is a constant, positive aft of the leading edge.	in
B	Bending flutter determinant element for $\alpha$	Non- Dimensional
C(k)	Theodorsen's Circulation function, equal to $F(k) + i \cdot G(k)$	Non- Dimensional
CG	Location of section center of gravity, positive aft of leading edge.	in
$C_l$	Section lift coefficient	Non- Dimensional
$C_{l\alpha}$	Section lift curve slope	$\frac{1}{\text{rad}}$

D	Torsional flutter determinant element for $h/b'$	Non- Dimensional
DOF	Degree of freedom	Non- Dimensional
E	Torsional flutter determinant element for $\alpha$	Non- Dimensional
EA	Location of section elastic axis, positive aft of leading edge	in
EOM	Equation(s) of Motion	
F(k)	Real part of Theodorsen's function	Non- Dimensional
iG(k)	Imaginary part of Theodorsen's function	Non- Dimensional
H <sub>cg</sub>	Section mass moment of inertia per unit span about center of gravity	slug·in <sup>2</sup>
H <sub>ea</sub>	Section mass moment of inertia per unit span about elastic axis	slug·in <sup>2</sup>
Im	Imaginary part of complex number	Non- Dimensional
J <sub>0</sub>	Zeroeth order Bessel function of the first kind	
J <sub>1</sub>	First order Bessel function of the first kind	
K <sub>T</sub>	Section torsional stiffness per unit span	$\frac{\text{lbf}}{\text{rad}}$
KTAS	Knots True Air Speed	knots

L	Lift force acting perpendicular to the airstream at the AC, per unit span, positive up.	lbf
$L_h$	Lift force coefficient due to bending oscillations per unit span using unsteady aerodynamics	Non-Dimensional
$L_\alpha$	Lift force coefficient due to torsional oscillations per unit span using unsteady aerodynamics	Non-Dimensional
LE	Abbreviation for the leading edge of the airfoil section	Non-Dimensional
M	Aerodynamic moment about the AC per unit span	Non-Dimensional
$M_h$	Aerodynamic moment coefficient due to section bending oscillations per unit span using unsteady aerodynamics	Non-Dimensional
$M_\alpha$	Aerodynamic moment coefficient due to section torsional oscillations per unit span using unsteady aerodynamics	Non-Dimensional
QS	Abbreviation for "Quasi-Steady"	
Re	Real part of complex number	Non-Dimensional
S	Section strip area	$\text{in}^2$
$S_\alpha$	Section static imbalance per unit span, equal to $m \cdot b' \cdot x_\alpha$	slug · in
T	Kinetic energy	lbf · in
U	Strain energy	lbf · in
US	Abbreviation for "Unsteady"	$\frac{\text{in}}{\text{sec}}$ , knots

V	Airstream velocity, a true airspeed	
V <sub>D</sub>	Static divergence speed	$\frac{\text{in}}{\text{sec}}$ , knots
V <sub>fl</sub>	Critical flutter speed, the speed at which the oscillations of the section occur at constant amplitude, using unsteady aerodynamics	$\frac{\text{in}}{\text{sec}}$ , knots
V <sub>fQS</sub>	Critical flutter speed using quasi-steady aerodynamics	$\frac{\text{in}}{\text{sec}}$ , knots
W <sub>t</sub>	Section weight per unit span	lbf
X	Square of the real part of the flutter frequency ratio, equal to $\left(\frac{\omega_T}{\omega_{fl}}\right)^2$	$\left(\frac{\text{rad}}{\text{sec}}\right)^2$
Y <sub>0</sub>	Zeroeth order Bessel function of the second kind	
Y <sub>1</sub>	First order Bessel function of the second kind	
Z	Square of the real and imaginary parts of the flutter frequency ratio, equal to $\left(\frac{\omega_T}{\omega_{fl}}\right)^2 \cdot (1 + i \cdot g)$	$\left(\frac{\text{rad}}{\text{sec}}\right)^2$
α	Section angle of attack; torsional spring rotation; second (rotational) degree of freedom, positive leading edge up.	radians, degrees
δ	Density ratio, equal to $\frac{\rho}{\rho_0}$	Non- Dimensional

$\delta W$	Virtual work of wing bending and torsion	lbf · in
$\mu$	Mass ratio of the airfoil section to a cylinder of air circumscribed about the section chord, equal to $\frac{m}{\pi \rho \cdot b^2}$	Non- Dimensional
$\rho$	Air density at test condition pressure and temperature	$\frac{\text{slug}}{\text{in}^3}$
$\rho_0$	Air density at International Standard Atmosphere pressure and temperature	$\frac{\text{slug}}{\text{in}^3}$
$\phi$	Phase angle between the bending and torsional DOF	rad , deg
$\omega_{fl}$	Coupled flutter frequency using unsteady aerodynamics	$\frac{\text{rad}}{\text{sec}}$
$\omega_{fQS}$	Coupled flutter frequency using quasi-steady aerodynamics	$\frac{\text{rad}}{\text{sec}}$
$\omega_b$	Uncoupled natural bending frequency in the vertical plane	$\frac{\text{rad}}{\text{sec}}$
$\omega_T$	Uncoupled natural torsional frequency about the elastic axis	$\frac{\text{rad}}{\text{sec}}$
•	Differentiation with respect to time	
	Aerodynamic center	
	Center of gravity	
	Elastic axis	

$\begin{pmatrix} \blacksquare \\ \blacksquare \end{pmatrix}$  Column matrix

$(\blacksquare \blacksquare)$  Row matrix

$\begin{pmatrix} \blacksquare & \blacksquare \\ \blacksquare & \blacksquare \end{pmatrix}$  Square matrix

$\left| \begin{pmatrix} \blacksquare & \blacksquare \\ \blacksquare & \blacksquare \end{pmatrix} \right|$  Determinant

## **Chapter 1.0: Introduction**

This thesis is intended to explain one type of the aeroelastic phenomenon known as flutter. The thesis examines two methods for determining the bending-torsion flutter frequency and speed of a one-dimensional, two degree-of-freedom airfoil section. It points out the assumptions, approximations and errors inherent in these methods, and demonstrates their use to determine the flutter frequency and speed of six example airfoil sections. Finally, the thesis examines the effects of changing the section Center of Gravity (CG) location on the flutter frequency and speed of the six airfoil sections.

### 1.1 Motivation for the thesis

A good deal of information about flutter is readily available in the literature. However, there is a need for an engineering analysis of the fundamental flutter mechanism combined with a convenient calculation program (in this case, a Mathcad 11 worksheet) that includes as program inputs all of the critical characteristics of an airfoil section and produces as the output the critical flutter frequency and speed. The critical flutter speed is the speed of airflow that will result in simple harmonic vibration of the airfoil section, where the amplitude of vibration is neither increasing

nor decreasing. The critical flutter frequency is the coupled frequency of vibration that accompanies this condition. To provide a meaningful comparison of the effects of using quasi-steady or unsteady aerodynamic forces, this methodology must calculate the flutter frequency and speed using both methods of defining the aerodynamic forces and moments. (Section 3.6 provides details of the aerodynamic forces and moments for each case.) This thesis seeks to fulfill this requirement by providing a parallel analysis of flutter characteristics for all six airfoil sections.

## 1.2 Objectives of the thesis

The four primary goals of this thesis are: 1) To show how the elastic, inertial and aerodynamic forces and moments acting on a one-dimensional airfoil section in two-dimensional airflow interplay to produce bending-torsion flutter; 2) To demonstrate two methods of calculating the critical flutter frequency and speed by the use of a programmed Mathcad 11 worksheet; 3) To determine the critical flutter frequency and speed of six example sections and compare the results of using quasi-steady and unsteady aerodynamic forces; and 4) To study the effects of Center of Gravity shift along the section chord for each section.

### 1.3 Thesis Organization

In support of these primary goals, Section Two provides a description of the basic characteristics of flutter, with a particular emphasis on those which distinguish it from other types of vibrations. The characteristics of the basic model and its limitations are described. Section Three derives two solution methods for determining the flutter frequency and speed. Lagrange's Equation provides the basis for the equations of motion. With the applicable quasi-steady or unsteady aerodynamic forces, the characteristic equation is produced. In both force cases, the solution to this equation yields the flutter frequency and speed. Additionally, the approximations, assumptions, limitations and sources of error in each of the two methods are identified and explained. Section Four examines six example sections, with the flutter frequency and speed calculated using both quasi-steady and unsteady aerodynamic forces. In support of the Center of Gravity study, plots of flutter speed as a function of CG position are provided for both cases.

### 1.4 Chapter Summary

It is hoped that this thesis will provide an overall understanding of what flutter is, how the critical flutter frequency and speed may be

mathematically determined, and how the structural, inertial, and aerodynamic parameters of the section determine the critical flutter frequency and speed. Through knowledge of these relationships, better design choices are made and greater understanding of flutter is promoted.

## **Chapter 2.0: A Fundamental Description of Flutter**

Many people have had firsthand opportunity to observe the phenomenon of aeroelasticity, which is the structural deformation of an airframe due to aerodynamic forces. For example, as an airline passenger, one frequently witnesses the bending of the aircraft wing while in flight. A less obvious aerodynamic structural deflection of the airframe, not so readily observed but equally real, is the torsional rotation of the wing under the same conditions. It is the relationship between the bending and torsional motions of the wing that is the basis for bending-torsion flutter.

### 2.1 Types of Aeroelasticity

To fully appreciate the forces and structural responses involved in flutter, it is important to distinguish it among the different types of possible aeroelasticity phenomena. Figure 2.1, adapted from Reference 17, illustrates the multiple relationships that exist among the forces and responses involved in static and dynamic aeroelasticity.

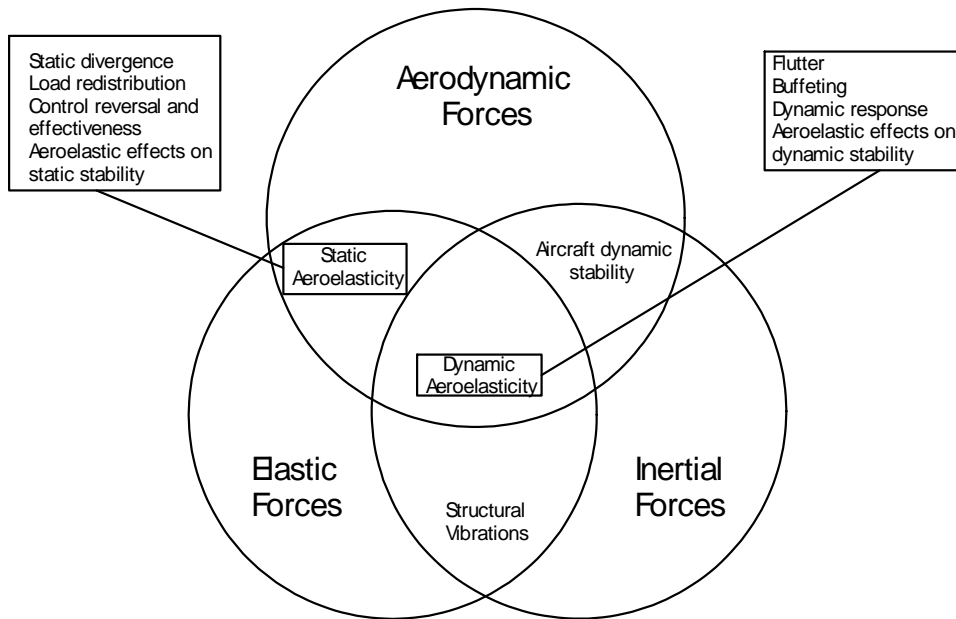


Figure 2.1: Summary of forces and responses.

This diagram is helpful in discerning between flutter (a dynamic structural response characterized by divergent oscillations) and the other types of aeroelastic structural responses possible, such as structural vibrations and static aeroelasticity. The main difference is that flutter involves the interplay of all three forces shown (elastic, inertial, and aerodynamic), where the structural response is, as a function of the speed of the airflow, in the form of a harmonic (constant amplitude) oscillation or a divergent oscillation of the structure.

Since aircraft structures must be light, they are flexible. Additionally, the thin airfoils sections required for high design speeds

encourage flexibility. This lack of stiffness leads to vibration, simply defined as any periodic motion of the structure. Vibration is the origin of flutter. A vibratory mode is a particular way all the components of the airframe structure vibrate at the same frequency. The vibratory modes of a given aircraft are often identified through a combination of analysis and ground vibration tests. After predicting the natural frequencies of vibration analytically, the ground vibration tests confirm the actual natural frequencies arising as a function of the configuration of the airplane. A conventionally configured airplane is defined in this thesis as a braced or cantilever monoplane with the tail assembly located at the aft end of the fuselage. In such an airplane, the combination of bending and torsional vibrations of the wings, fuselage and control surfaces lead to the most common forms of flutter, as described below. After the vibratory modes are determined, the analyst decides what degrees of freedom (DOF) will be necessary in a given analysis, and then uses generalized coordinates to mathematically define the motions of the structure. A generalized coordinate is defined as any coordinate required to completely specify the configuration of the system at any particular time.

Coupling unites the motions of the DOF to produce a new, unique coupled frequency of vibration, which is a function of the elastic, inertial and aerodynamic forces and moments in combination within the structure.

Thus, the vibratory modes of the components of the airframe are the foundations of the structural vibrations that lead to flutter. Vibration itself is not flutter, but vibration, combined by coupling to affect energy transfer from the airstream, is required for two degree-of-freedom flutter to occur. This important distinction is made by Figure 2.1, since unforced structural vibrations alone are not the equivalent of flutter, because they lack the component of aerodynamic forces. Similarly, static divergence lacks the inertial component, as it involves only aerodynamic and elastic forces. Although it shares many of the forces seen in flutter in its basic mechanics, it must be distinguished from flutter since it is not a dynamic aeroelastic phenomenon. Only flutter, and the other forms of dynamic aeroelasticity shown, combine all three forces in the structural response.

## 2.2 Distinctive Characteristics of Classical Airfoil Section Flutter

Certain characteristics of the classical flutter of an airfoil section may be identified. In this thesis, the flutter of a flag, or that of other systems which involve large deflections, is not considered. Examples of these excluded types of flutter are stall flutter, vortex shedding from bluff bodies, and the effects of flow separation on structures. This discussion is limited to the small deflections of a one-dimensional airfoil section in two-dimensional potential (unseparated) flow. Such flutter is:

-a self-exciting phenomenon, where the airfoil's own deflections induce the aerodynamic forces and moments that lead to further deflections;

-determined by the interplay of elastic, inertial and aerodynamic forces;

-dependent on the energy balance between the immediate airstream and the airfoil structure, and the subsequent energy transfer from the airstream to the structure;

-dependent on the phasing of the various motions of the structure;

-a dynamic instability, defined by a particular critical velocity of the airstream, at which the energy transferred from the airstream is equal to the structural damping. Stability is defined as the tendency of the system to return to a state of equilibrium following a disturbance. As the problem is mathematically a stability problem and not one of forced response, this critical stability condition defines a stability boundary. The boundary may be located by finding the solution to the system of the linear differential equations of motion of the section, as it vibrates in simple harmonic motion.

-determined by the values of specific parameters, including:

-the locations of the section aerodynamic center (AC), center of gravity (CG), and elastic axis (EA);

-the section mass, and therefore its weight;

-the section mass moment of inertia about the elastic axis ( $H_{ea}$ ) and therefore the distribution of that weight, and,  
-the section elastic properties, as defined by the bending ( $k_b$ ) and torsional ( $K_T$ ) stiffnesses.

Thus, to understand exactly what flutter is, it is important to recognize what it is not. Flutter must be distinguished from simpler forms of vibration. The critical concept is the existence, for this simple system, of at least two degrees of freedom, which, due to the effects of increasing velocity, become mutually reinforcing through the phasing of their motions. Flutter, in its fully developed state, is a divergent structural response. As such, the magnitude of the structural deflections increases without bound as time progresses. This is to be distinguished from the case of non-divergent structural vibrations, which do not constitute flutter because of the decreasing amplitude of deflections observed over time.

### 2.3 Types of Airfoil Section Flutter

The range of possible modes by which flutter may occur is extensive, limited only by the configuration of the airframe and its vibratory modes. A few examples of the combinations of vibratory modes that typically lead to flutter are discussed below.

### 2.3.1 Vibratory modes

For airplanes of conventional configuration, some examples of possible combinations of natural vibratory modes which may lead to flutter include wing bending and torsion, fuselage bending and torsion, stabilizer bending and torsion, and control surface deflection modes. The flutter may be symmetric or anti-symmetric about the primary axes of the aircraft.

### 2.3.2 Examples of Airfoil Section Flutter with Increasing Numbers of Types of Motion

Flutter modes involving two types of motion (binary flutter) are typified by wing bending-torsion, fuselage bending-elevator rotation, fuselage torsion-rudder rotation, fuselage torsion-elevator rotation, and stabilizer bending-torsion flutter. For flutter involving three types of motion (ternary flutter), a control surface frequently provides the additional component of movement. Examples are wing bending-torsion-aileron rotation, fuselage bending-rudder-tab rotation, fuselage bending-elevator-tab rotation, fuselage torsion-rudder-tab rotation, fuselage torsion-elevator-tab rotation, and stabilizer bending-torsion-elevator rotation. Flutter involving four types of motion requires four components capable of movement. Two examples of such flutter are wing bending-torsion-

aileron-tab rotation and stabilizer bending-torsion-elevator-tab rotation flutter. This list is intended to give a few examples of typical types of flutter possible on an aircraft of conventional configuration. It is by no means all-inclusive. Any two vibratory modes may theoretically combine to produce flutter if input energy and coupling are available. Binary flutter is the basis for all higher flutter modes, such as those involving control surfaces and tabs. It is for that reason examination of the binary case provides an adequate basis for understanding all flutter types and their solution methodologies.

#### 2.4 Bending-torsion Flutter of an Airfoil Section as Described in this Thesis

The model used in this thesis describes an airfoil section, as representative of a complete wing, in bending-torsion flutter. It cannot be used to confidently evaluate the flutter characteristics of an entire wing, but can give insights into the fundamental mechanism of flutter. Figure 2.4 is a diagram of the one-dimensional (having the dimension of the chord length,  $c$ , only) airfoil section, showing the two degrees of freedom of motion:  $h$ , the vertical displacement; and  $\alpha$ , the torsional displacement (Donaldson, 1993). These degrees of freedom are further discussed in Section 2.4.1. Also, the locations of the aerodynamic center (AC), the

center of gravity (CG), and the elastic axis (EA) of the two-dimensional section are shown. The airstream velocity ( $V$ ), the lift force ( $L$ ) generated by the section, the aerodynamic moment ( $M$ ) and the bending and torsional stiffnesses are seen. These parameters represent the properties of the system and in combination determine its dynamic response. Since this model represents an airfoil section, it is necessary to make some assumptions in order to estimate the flutter properties of an entire wing. The elastic (bending and torsional stiffness), inertial (mass and mass distribution), and dimensional (section chord length) properties of the entire infinite span, untapered wing are represented by those properties found at the 70-75% wing semi-span position. This “rule of thumb” is the result of observation in testing of actual aircraft wings (Bisplinghoff, Ashley, and Halfman, 1955). Since the wing is assumed to be of constant cross section, at all points along the span, the sections are identical and the stiffnesses are constant. They are assumed to be perfectly linear, with the elastic restoring forces directly proportional to the structural displacements. Also, the structure is perfectly elastic, in that it will return completely to its original shape after load application and removal. Since the work of deformation is completely converted into strain energy, the elastic forces are conservative, as no frictional losses due to internal structural damping occur.

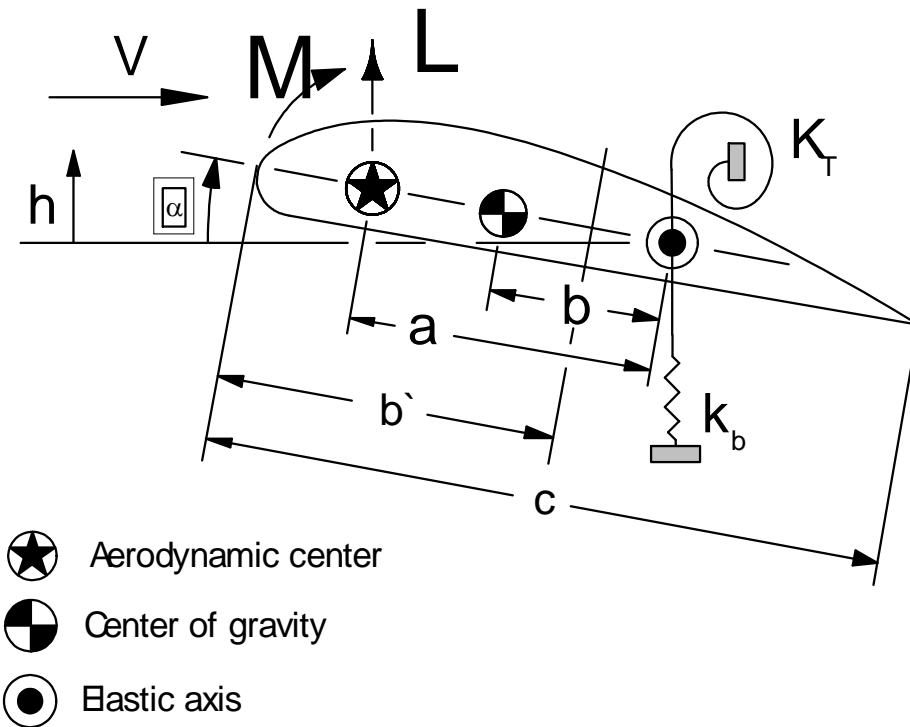


Figure 2.4. Two degree of freedom model for bending-torsion flutter.

#### 2.4.1. Defining the Degrees of Freedom

In bending-torsion flutter, two fundamental vibratory modes may occur. One is wing vertical bending, and the other is wing torsion about the wing's elastic axis. The two generalized coordinates required to completely and unambiguously describe the vibratory motions of this thin, one-dimensional airfoil section (a "thin" foil section is one having an infinitesimal thickness to chord ratio) in this two degree-of-freedom system

are (1) the section vertical translation,  $h$ , positive up for the quasi-steady case (and positive down for the unsteady case); and (2) the section rotation about the elastic axis,  $\alpha$ , positive leading edge up. The generalized coordinates specify the exact configuration<sup>3</sup> of the system at any time. The generalized coordinates are used with Lagrange's Equation to form the equations of motion of the system.

## 2.5 Chapter Summary

Flutter is a divergent, coupled oscillation. For clarity of understanding, one must be able to identify other types of vibrations and why they do not qualify as flutter since they lack one or more components of the three forces involved in flutter. This simple flutter model is adequate to the task of describing airfoil section flutter, but falls short of being able to represent an actual wing without the sacrifice of accuracy. The two degree of freedom model provides a complete description of the motions of the system through the generalized coordinates. These are then used with Lagrange's Equation to build the equations of motion.

This Page Intentionally Left Blank

## **Chapter 3.0: Solutions for the Flutter Frequency and Speed**

This section describes two elementary means by which the flutter frequency and speed may be found. By examining the derivation of the equations of motion and the solution of the resulting characteristic equation, the factors affecting the flutter solution are examined and explained. In the first case, aerodynamic forces are described by quasi-steady two dimensional (2-D) aerodynamics, while in the second, unsteady 2-D aerodynamics are used. In each, the assumptions and limitations of the respective method are described, and the errors evaluated.

As the objective of this thesis is to bring about an understanding of flutter, the process of determining the equations of motions and finding the solution to the flutter frequency and speed is essential. Examining and comparing these two solution methods, and the errors that arise from them, support the goal of developing a comprehensive understanding of flutter and the factors that affect it.

### **3.1 Derivation of the Lagrange Equations of Motion**

Solution of the classical two-degree-of-freedom bending-torsion flutter problem requires the solution of a system of second-order

linear differential equations of motion. By arranging this system of equations with the appropriate aerodynamic forces in matrix form, and requiring the resulting determinant to equal zero, a characteristic equation results. The roots of this characteristic equation are then used to determine the flutter frequency and speed. This solution method is limited to small displacements due to the requirement that the equations of motion be linear. This is a result of the requirement that the elastic properties and the aerodynamic lift curve slope be linear.

Lagrange's Equation, a restatement of Newton's Second Law, provides the basis for forming the equations of motion using energy terms.

Lagrange's equation, in general, is:

$$\frac{d}{dt} \left( \frac{\partial T}{\partial \dot{q}_i} \right) - \frac{\partial T}{\partial q_i} + \frac{\partial U}{\partial q_i} = Q_i$$

where  $q_i$  is the  $i$ th generalized coordinated,  $T$  is the kinetic energy,  $U$  is the strain energy, and  $Q_i$  is the  $i$ th generalized external force (Scanlon, Rosenbaum, 1968).

To write the Lagrange equations of motion, the kinetic energy and strain energy of the oscillating section are required. These are easily obtained from inertial and elastic forces. The external generalized forces,

which in this case will be aerodynamic forces and moments, are then determined by calculating the virtual work of bending and torsion. After taking the appropriate derivatives and determining the generalized forces, these values are substituted into Lagrange's equation and the system of the equations of motion is formed.

### 3.1.1 Strain Energy of Elastic Forces

Hooke's Law is the constitutive law of the strain energy of the elastic forces when the deflections are small. In terms of the DOF's  $h$  and  $\alpha$ , the strain energy is (Hurty, Rubinstein, 1964):

$$U = \frac{1}{2} \cdot k_b \cdot h^2 + \frac{1}{2} K_T \cdot \alpha^2$$

### 3.1.2 Kinetic Energy of Inertial Forces

The kinetic energy represents the inertial energy of the system (Bisplinghoff, Ashley, and Halfman, 1955):

$$T = \frac{1}{2} m \cdot (\dot{h} + b \cdot \dot{\alpha})^2 + \frac{1}{2} \cdot H_{cg} \cdot \dot{\alpha}^2$$

or,

$$T = \frac{1}{2} \cdot m \cdot \dot{h}^2 + \frac{1}{2} \cdot (H_{cg} + m \cdot b^2) \cdot \dot{\alpha}^2 + m \cdot b \cdot \dot{h} \cdot \dot{\alpha}$$

### 3.1.3 Generalized Forces

The non-conservative external forces applied to the system are the aerodynamic forces and moments. The generalized forces and moments in this system are calculated by determining the work done during a virtual displacement of each one of the generalized coordinates, while the other generalized coordinates remain undisplaced. To obtain the generalized forces and moments acting on the airfoil section, the virtual work ( $\delta W$ ) of the section is calculated. In terms of DOF's  $h$  and  $\alpha$ , the virtual work is the summation of work associated with the bending and torsional motions (Bisplinghoff, Ashley, and Halfman, 1955):

$$\delta W = \delta W_h + \delta W_\alpha$$

For small bending displacements, Lift is the applied force:

$$\delta W_h = L \delta h$$

$$Q_h = L$$

For small torsional displacements, the product of Lift and the moment arm ( $a$ ) is the applied moment. As discussed in section 3.6.4.1,

in the case of quasi-steady 2-D aerodynamics, the aerodynamic moment is a static moment and thus is omitted from this calculation of dynamic forces:

$$\delta W_{\alpha} = L \cdot a \cdot \delta \alpha$$

$$Q_{\alpha} = L \cdot a$$

The total virtual work of the section is described by the superposition of the bending and torsional virtual work:

$$\delta W = L \delta h + L \cdot a \cdot \delta \alpha$$

The detailed description of the quasi-steady and unsteady aerodynamic forces will be provided in sections 3.6.4 and 3.6.5. These forces and moments will then be applied as appropriate to Lagrange's Equation to complete the equations of motion, as applicable.

### 3.2 Writing the Lagrange Equations of Motion

In preparation for substitution into Lagrange's equation, we now take the partial derivatives of the strain energy with respect to DOF's  $h$  and  $\alpha$  :

$$\frac{\partial}{\partial h} U = k_b \cdot h$$

$$\frac{\partial}{\partial \alpha} U = K_T \cdot \alpha$$

Similarly, taking the partial derivatives of the kinetic energy with respect to DOF's  $h$  and  $\alpha$ ,

$$\frac{\partial}{\partial h} T = m\dot{h} + mb\dot{\alpha}$$

$$\frac{\partial}{\partial \alpha} T = mb\dot{h} + mb^2\dot{\alpha} + H_{cg} \cdot \alpha$$

Taking the time derivative of the variation of the kinetic energy with respect to DOF's  $h$  and  $\alpha$ ,

$$\frac{d}{dt} \left( \frac{\partial}{\partial h} T \right) = m\ddot{h} + mb\ddot{\alpha}$$

$$\frac{d}{dt} \left( \frac{\partial}{\partial \alpha} T \right) = mb\ddot{h} + mb^2\ddot{\alpha} + H_{cg} \cdot \ddot{\alpha}$$

Since  $T$  contains no  $h$  or  $\alpha$  terms,

$$\frac{\partial}{\partial q_i} T = 0$$

Substituting each of the above results into Lagrange's equation,

and including the generalized aerodynamic forces, the equations of motion are:

$$m \cdot \ddot{h} + m \cdot b \cdot \ddot{\alpha} + k_b \cdot h = L$$

$$m \cdot b \cdot \ddot{h} + (H_{CG} + mb^2) \cdot \ddot{\alpha} + K_T \cdot \alpha = M$$

or, using the mass moment of inertia about the section elastic axis, the second equation of motion becomes

$$H_{ea} = H_{CG} + mb^2 ;$$

$$m \cdot b \cdot \ddot{h} + H_{ea} \cdot \ddot{\alpha} + K_T \cdot \alpha = M$$

Inertial coupling may be readily observed in this system of equations of motion. The coupling terms are  $m \cdot b \cdot \ddot{\alpha}$ , which couples torsion to the bending equation of motion, and  $m \cdot b \cdot \ddot{h}$ , which couples bending to the torsional equation. Inertial de-coupling therefore occurs when the “b” term, the lever arm distance from the Center of Gravity (CG) to the Elastic Axis (EA), is zero. This is, of course, the case when the CG and the EA are co-located.

### 3.3 Energy Transfer and Coupling

Energy transfer is required for flutter to occur, and coupling is the means by which energy transfer is facilitated. Flutter cannot occur if either coupling or energy transfer is absent.

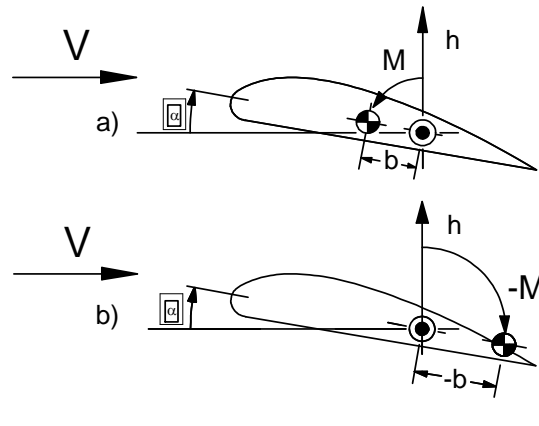
#### 3.3.1 Energy Transfer from the Airstream

The fundamental driver of flutter is the energy transfer from the airstream to the structure via coupling of the two degrees of freedom. The balance of the energies in the system, elastic (strain), inertial (kinetic), and aerodynamic (kinetic), governs the speed at which flutter will occur. If viewed as a flutter engine, the wing can be observed to do net work on the airstream, or to have the airstream do net work upon it. (Fung, 1969). In the stable condition, the wing is doing net work on the airstream. In this case, the elastic and inertial energies of the oscillating structure exceed the energy input of the airstream. In the critical flutter condition, the energies of the airstream (aerodynamic) and the structure (elastic and inertial), are exactly balanced. In the full flutter condition, the airstream is doing positive net work on the structure, since the aerodynamic energy input of the airstream exceeds the elastic restoring energy of the structure together with its inherent inertial energies. Coupling is the interaction of

the two degrees of freedom which serves as the path by which energy transfer occurs. In this system, both inertial and aerodynamic coupling are present.

### 3.3.2 Inertial coupling due to Center of Gravity location

In inertial coupling, the location of the section center of gravity (CG), determines whether the section's flutter properties will be enhanced (higher flutter speed) or diminished (lower flutter speed). Figures 3.3.2 (a) and (b) demonstrate the combinations of the bending motion, the torsional deflection and the inertial moment. In Figure 3.3.2 (a), the CG is located ahead of the EA (defined here as "positive" inertial coupling). When the section is displaced upward in bending, the inertial moment ( $M$ ) opposes torsional rotation, reducing the angle of attack and thus the lift force. Figure 3.3.2(b), defined as "negative" inertial coupling, demonstrates the effect of the CG when it is located aft of the EA. When the section is vertically displaced upward, the inertial moment ( $-M$ ) acts to increase the torsional deflection. Such torsional deflections, by increasing the angle of attack, lead to generation of greater aerodynamic forces and further bending and torsional deflections. This is a very pro-flutter condition.



$M$  Inertial moment

Figure 3.32. Inertial coupling as a function of CG position.  
 a) Positive b) Negative.

### 3.3.3 Phasing of the Motions

Phasing, (the variation of the phase angle between the degrees of freedom as a function of coupling) is the result of combining the elastic, inertial, and aerodynamic forces in such a way so as to either suppress or encourage flutter. The phase angle indicates whether the motions of each separate DOF opposes or reinforces the other's deflections.

### 3.3.4 Aerodynamic Coupling via Phasing

Aerodynamic coupling may occur as the result of the action of either the bending or torsional degree of freedom. The aerodynamic coupling resulting from the action of the bending degree of freedom is

always stable. When the wing is bending down, the effective angle of attack is increased by the vertical velocity, increasing the lift force, and assisting the elastic forces in restoring the wing to its point of zero vertical displacement. Conversely, when the wing is bending up, the upward velocity reduces the effective angle of attack. This decreases the lift force, and once again helps the elastic forces restore the wing to its point of zero vertical displacement.

Aerodynamic coupling of the torsional degree of freedom can be stabilizing, neutral, or destabilizing, depending on the phase angle between the bending and torsional degrees of freedom. An example of the stable condition is when the phase angle is 180 degrees. Such a case occurs when the angle of attack is at its maximum negative value when the bending is at its maximum positive value. The stable condition exists when the phase angle is from 180 to just over 90 degrees. The neutral (critical flutter) condition occurs when the phase angle is precisely 90 degrees, where the torsional displacement (angle of attack) is maximum when the bending displacement is zero; and zero when the bending displacement is maximum (Fung, 1968). This condition is marked by the sinusoidal, harmonic motions of the DOF's. The unstable full flutter condition occurs as a result of aerodynamic coupling when the phase angle is less than 90 degrees. In this condition, the angle of attack

increases as the bending increases, leading to further bending, and so on. In this divergent condition, the amplitudes of the DOF's can increase rapidly, leading to structural failure in a few cycles of motion.

Torsion is the unstable vibratory mode in this system, and it is through the torsional DOF that energy passes to the bending mode. This is the energy transfer that leads to structural failure as the divergent cycle in the full flutter condition progresses (Fung, 1969).

### 3.4 Frequency Coalescence

Frequency coalescence, or the convergence of the coupled frequencies of each DOF towards each other, is also exhibited in flutter. Fundamental to the process is the uncoupled natural frequency of each DOF. In a two-degree-of-freedom system, there are two natural, uncoupled frequencies of vibration. These two distinct frequencies are functions of, for bending, the bending stiffness and the mass; and for torsion, the torsional stiffness, and the mass moment of inertia. As the velocity of the airflow increases and the energy input to the system increases, the coupled vibratory frequency of each DOF converges towards, or coalesces upon, a common coupled flutter frequency. The flutter frequency determined by the Mathcad worksheet,  $\omega_{fQS}$  or  $\omega_{fl}$ , is

this coupled frequency.

### 3.5 Phasing Diagrams

Three phasing diagrams are provided below to depict the process of phase shift as the velocity of the airflow increases and frequency coalescence occurs. In each diagram, the stable, critical, and unstable flutter conditions are depicted.

#### 3.5.1 Stable Condition

The stable condition is depicted in Figure 3.5.1, a phase and frequency diagram of the vertical and torsional oscillations of the section, where the coupled frequency ratio of the bending oscillation to the torsional oscillation is equal to 0.5. In other words, the cyclic torsional motion is twice as fast as the cyclic vertical motion. The diagram shows that the torsional oscillation completes two cycles, from zero deflection, to positive maximum, to zero, and negative maximum and back to zero, in the same amount of time that the vertical oscillation completes one full cycle.

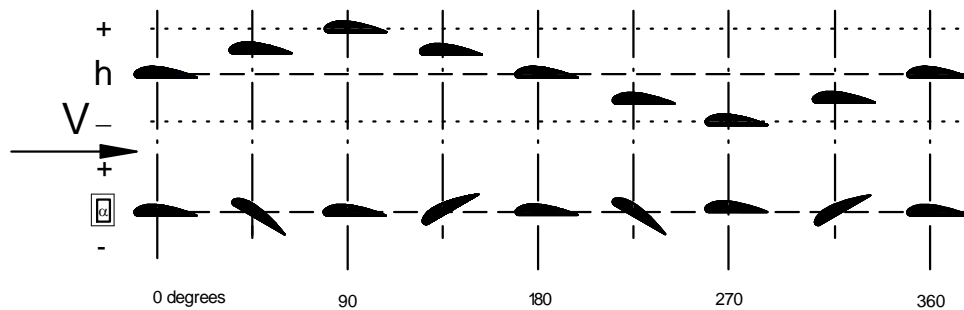


Figure 3.5.1. Stable vertical and torsional oscillations, where the natural torsional frequency is equal to twice the natural bending frequency (Frequency ratio equal to 0.5).

As airflow velocity increases, the stable bending mode coupled frequency remains relatively constant, but the unstable torsional coupled frequency decreases. This occurs as the strength of the “aerodynamic spring” approaches the torsional stiffness of the wing as a result of the increased aerodynamic force (Fung, 1969). The torsion to bending frequency ratio thus reduces, in this example, from 2.0 to approaching unity.

### 3.5.2 Critical Flutter Condition

The critical flutter condition is shown in Figure 3.5.2, a phase and frequency diagram of the DOF oscillations where the motions are 90 degrees out of phase and the frequency ratio is 1.0, in the condition of frequency coalescence. In this diagram, the two DOF's are reaching their maximum displacements, either positive or negative, at different times (90

degrees out of phase), while the coupled frequencies of the bending and torsional oscillations are equal or nearly equal. Any increase in velocity will cause the phase angle between the DOF's to become less than 90 degrees, allowing aerodynamic coupling, and hence divergent oscillations, to occur. This phase shift occurs quite rapidly as the coupled frequency ratio approaches unity. In fact, in the case of no damping, as assumed in this case, the phase shift is instantaneous (Scanlon, Rosenbaum, 1968).

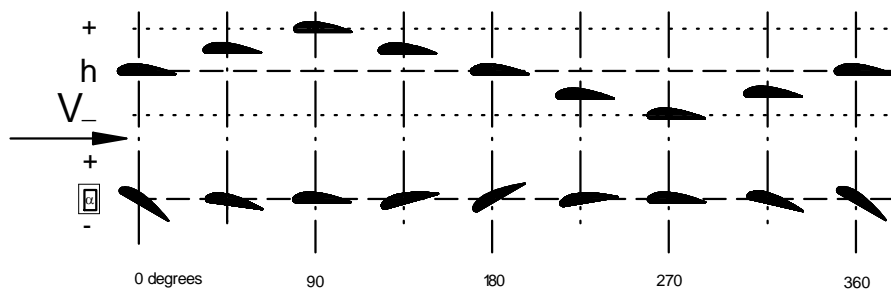


Figure 3.5.2: Critical flutter (stability boundary) condition, where the vertical and torsional oscillations are 90 degrees out of phase, and where the coupled torsional frequency nearly equals the coupled bending frequency (Frequency Coalescence).

### 3.5.3 Full Flutter Condition

In the unstable full flutter condition, both degrees of freedom are reaching their maximum displacements at the same time (moving in-phase), and each DOF is aerodynamically reinforcing the motions of the other. Figure 3.5.3 is a phase and frequency diagram of the full flutter condition, where the two DOF's are moving in-phase and at the same coupled frequency. Such angular displacement at its maximum tends to

drive the vertical displacement  $h$  even higher with each cycle.

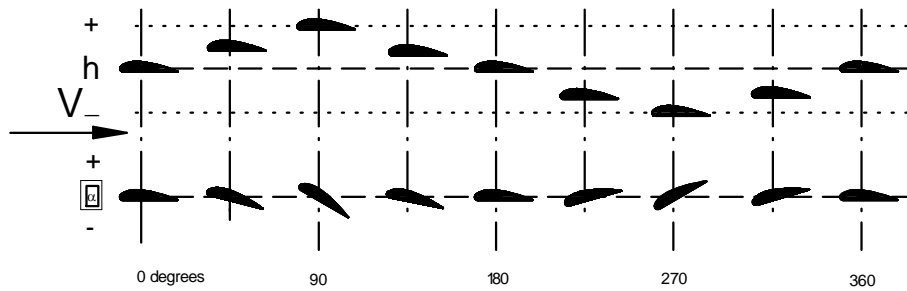


Figure 3.5.3. Full flutter condition, where the vertical and torsional oscillations are moving in phase at the flutter frequency.

### 3.6 Aerodynamic Forces

All of the aerodynamic forces and moments generated by the section arise only as a result of the section's oscillation. The aerodynamic forces and moments included in this analysis are thus limited to dynamic forces and moments, and any static forces and moments required to maintain equilibrium are excluded (Scanlon, Rosenbaum, 1968).

Also, in both the quasi-steady and unsteady cases, a number of simplifying assumptions regarding the air have been made. Fluid properties, two-dimensional flow and lift curve slope are all simplified as follows.

### 3.6.1 Fluid Properties

In this analysis, the air is considered to be a perfect fluid. As such, the air is an inviscid (frictionless) fluid, leading to an overstatement of the aerodynamic forces. The Reynolds Number, which is the non-dimensional ratio of the fluid's inertial forces to its viscous forces, is infinite. This means that at every point on the airfoil, no boundary layer is formed, so potential flow is assured, and no separation of the air from the airfoil occurs. The potential flow lift curve slope of the airfoil is also slightly overstated as a consequence. This fictitious efficiency of the airflow leads to an overstatement of the aerodynamic forces generated. The inviscid assumption also means that no drag forces are generated by this model (Milne-Thompson, 1958).

Also, since here the air is considered incompressible, no changes in air density occur as the flow velocity increases. The Mach Number, the ratio of the airflow velocity to the local speed of sound, is therefore zero. This assumption will limit the range of valid speeds to those below about 250 knots. This non-conservative error would progressively degrade the accuracy of flutter speed predictions at higher speeds.

Environmental conditions are assumed to be International Standard

Atmospheric (ISA) conditions of sea level pressure and the standard temperature of 15 degrees centigrade. Neglecting compressibility effects, the flutter speed, as a true airspeed, is inversely proportional to the density ratio (the ratio of the density of air at a given altitude to the standard air density), and so a higher altitude, having a lower density ratio than sea level, results in a higher flutter speed. ISA conditions are thus the most conservative in terms of the resulting critical flutter speed. See Section 4.2.3 for an example of flutter calculations at increasing altitudes.

Finally, an inviscid fluid provides no fluid damping to impede the vibrations of the structure. This conservative error is considered acceptable due to the minimal amount of damping that would occur as the section oscillates in a real fluid, and also since the calculated critical flutter speed will be below the actual flutter speed. Basic section flutter behavior is not profoundly influenced by the lack of fluid damping, since flutter arises from the energy transfer that occurs via the coupling between the DOF, rather than from the energy dissipation that accompanies damping.

### 3.6.2 Basic strip theory

Two-dimensional (2-D) aerodynamic theory, where the flow occurs in the  $xy$  plane only, is used in both the Quasi-steady and Unsteady cases. Figure 3.6.2 depicts the external, non-conservative aerodynamic forces estimated by basic strip theory.

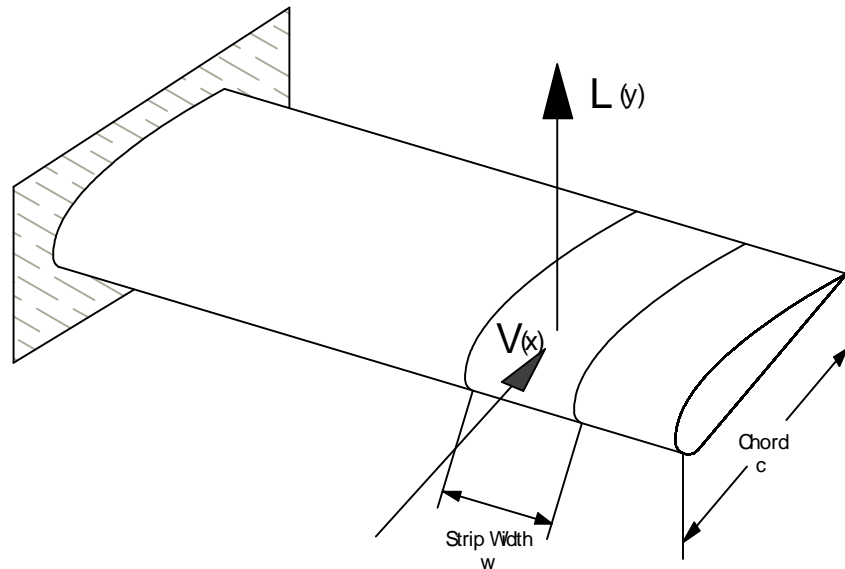


Figure 3.6.2. Basic strip theory.

Strip theory is a means of approximating the lift force generated by a wing of finite span using two-dimensional flow over a strip of arbitrary width. By dividing the wing into such strips, and then using two-dimensional flow properties to generate the lift force attributable to that

strip's width, vertical motion and local angle of attack, the strip's tributary lift force is determined. Adding the lift force of all the strips for the entire wing would yield the wing's total lift force, but would neglect the effects of true three dimensional flow, such as those resulting from tip vortices.

This one-dimensional structural model thus approximates a wing of infinite length. These assumptions cause conservative errors in the calculations of the aerodynamic forces since there is no accounting for interference effects of adjacent structures and flow patterns (Smilg, Wasserman, 1942).

### 3.6.3 Two Dimensional Airfoil Section Properties

The following table is provided as a reference of representative airfoil properties, where aerodynamic center (AC) location is in tenths of chord length, and where the lift curve slope and aerodynamic moment are per degree (Perkins, Hage, 1949):

<b>Section Number</b>	<b>AC Location</b>	<b>Lift Curve Slope</b>	<b>Aerodynamic Moment</b>
0009	0.250	0.110	0.000
1412	0.252	0.103	-0.023
2412	0.247	0.104	-0.040
4412	0.247	0.106	-0.090
23012	0.247	0.104	-0.013

64-012	0.262	0.110	0.000
64-412	0.267	0.112	-0.073
64-415	0.264	0.114	-0.070
64A212	0.262	0.108	-0.040
64A215	0.265	0.111	-0.037
65-212	0.261	0.108	-0.035
65-412	0.265	0.109	-0.070
65-415	0.268	0.107	-0.068

Table 3.6.3 Airfoil Section Properties

These two-dimensional properties include no corrections for finite span effects and are valid for a Reynolds Number of 6,000,000, and are thus appropriate for use in this two-dimensional analysis using basic strip theory. Aerodynamic center location is seen to be typically in the quarter-chord region, and the lift curve slope is assumed to be constant and linear within the small range of angle of attack (+/- 10 degrees). The rigid airfoil profile is considered to remain undeformed, and thus there is no variation in the lift force generated as a result of section deflections.

#### 3.6.4 Development of the Quasi-steady Aerodynamic Forces

In this thesis, the lift force is described in two fundamental ways. It may be considered as a force generated by the airfoil at a particular angle of attack, with the wing bending at a particular rate in a certain airstream

velocity, without regard for the fact that the airfoil section is torsionally oscillating in the flow. This is the basic scenario employed in quasi-steady 2-D aerodynamics, where the effects of the wake downstream of the airfoil are disregarded (Bisplinghoff, Ashley, 1962). As will be explained in Section 3.6.5.1, this results in an overstated lift force and a conservative calculation of the flutter speed.

#### 3.6.4.1 Aerodynamic Moment

An asymmetrical airfoil section generates changes in both the lift force and an aerodynamic moment (the pitching moment), about the quarter chord point, as a result of changes in the angle of attack while in an airflow. In quasi-steady 2-D aerodynamics, the lift force varies with time as the section oscillates vertically and torsionally. The quasi-steady lift therefore produces dynamic deflections and is thus included as a dynamic force in this analysis. The aerodynamic pitching moment of the airfoil, however, is essentially a constant with respect to changes in angle of attack, as demonstrated by the low value of the slope of the pitching moment coefficient in Figure 3.6.3 below. Therefore, in quasi-steady flow, the pitching moment is a static moment and is thus omitted from the aerodynamic forces and moments. The only moment attributable to aerodynamic forces in the quasi-steady analysis is that due to the

application of the section lift force ( $L$ ) at the distance ( $a$ ) from the elastic axis ( $EA$ ).

In unsteady flow, the section aerodynamic moment is a dynamic moment producing dynamic deflections as a function of the reduced frequency of oscillation of the section. The unsteady aerodynamic moment is not a static moment and is therefore included in the dynamic forces and moments acting on the oscillating section. Unsteady aerodynamic forces are further considered in Section 3.6.5.

Figure 3.6.3, from Reference 18, illustrates the low value of the aerodynamic moment curve slope for a NACA 23012 airfoil. Moreover, for symmetrical airfoil sections, the aerodynamic moment curve slope is zero.

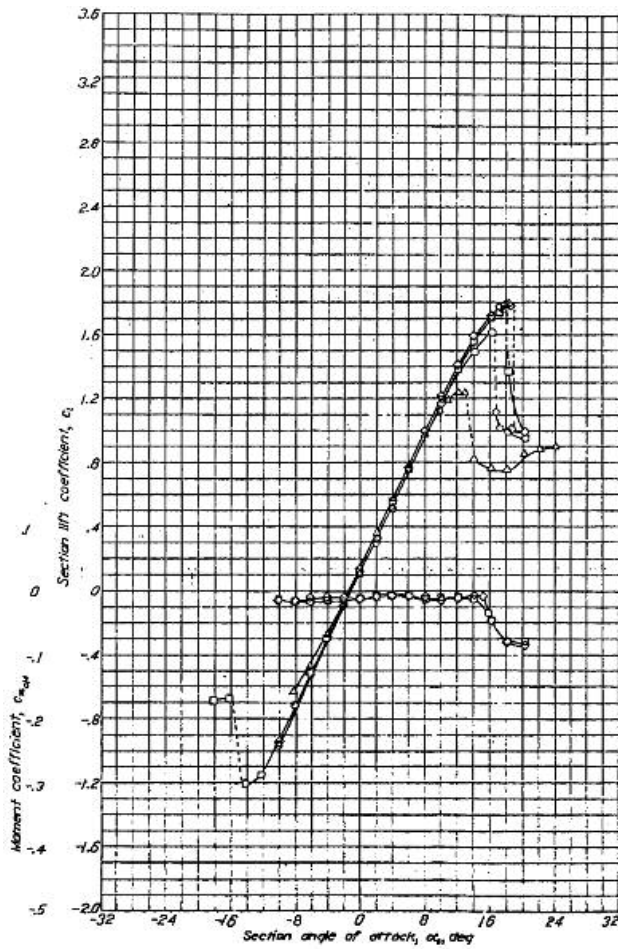


Figure 3.6.3 Lift curve and aerodynamic moment curve slopes

### 3.6.4.2 Forming the Lagrange Equations of Motion using Quasi-steady Aerodynamic Forces

The quasi-steady lift force ( $L$ ) of the airfoil section is defined as the product of dynamic pressure ( $q$ ), section planform area ( $S$ ), the quasi-steady lift curve slope ( $C_{l\alpha}$ ), and the angle of attack ( $\alpha$ ). Stating the

quasi-steady lift force as a function of time, and defining the effective lift force as a function of  $h$  and  $\alpha$  :

$$L(t) = \frac{1}{2} \cdot \rho \cdot S \cdot C_{l\alpha} \cdot V^2 \cdot \alpha_{\text{eff}}$$

where  $\alpha_{\text{eff}}$  is:

$$\alpha_{\text{eff}} = \alpha(t) - \frac{\dot{h}(t)}{V}$$

The above equation reflects the fact that the geometric angle of attack between the airstream and the section chord line is not the only variable important in determining the lift force. The vertical motion of the section affects the local angle of attack as well. Including the vertical translation of the airfoil section due to bending, the lift force becomes:

$$L = \frac{1}{2} \cdot \rho \cdot S \cdot C_{l\alpha} \cdot V^2 \cdot \left[ \alpha - \left( \frac{\dot{h}}{V} \right) \right]$$

Substituting for constants, the aerodynamic lift factor is:

$$A_0 = \frac{1}{2} \cdot \rho \cdot S \cdot C_{l\alpha}$$

The dynamic lift force resulting from bending and torsion is thus:

$$L = A_0 \cdot V^2 \cdot \left[ \alpha - \left( \frac{\dot{h}}{V} \right) \right]$$

$$L = A_0 \cdot V^2 \cdot \alpha - A_0 \cdot V \cdot \dot{h}$$

Adding this expression to the equations of motion completes the system of linear ordinary differential equations with constant coefficients for the quasi-steady case:

$$m \cdot \ddot{h} + m \cdot b \cdot \ddot{\alpha} + k_b \cdot \dot{h} = A_0 \cdot V^2 \cdot \alpha - A_0 \cdot V \cdot \dot{h}$$

$$m \cdot b \cdot \ddot{h} + (H_{cg} + mb^2) \cdot \ddot{\alpha} + K_T \cdot \alpha = a \cdot (A_0 \cdot V^2 \cdot \alpha - A_0 \cdot V \cdot \dot{h})$$

Rearranging and transposing, the homogeneous equations of motion for the quasi-steady case are:

$$m \cdot \ddot{h} + m \cdot b \cdot \ddot{\alpha} + A_0 \cdot V \cdot \dot{h} + k_b \cdot \dot{h} - A_0 \cdot V^2 \cdot \alpha = 0$$

$$m \cdot b \cdot \ddot{h} + H_{ea} \cdot \ddot{\alpha} + a \cdot A_0 \cdot V \cdot \dot{h} + (K_T - a \cdot A_0 \cdot V^2) \cdot \alpha = 0$$

### 3.6.5 Development of the Unsteady Aerodynamic Forces

The alternative to quasi-steady flow is to account for the torsional oscillations of the airfoil in the calculation of the lift force. In that case, unsteady 2-D aerodynamics is used, where the magnitude of the lift force is dependent on the frequency of the oscillation of the airfoil section. The

unsteady lift force is a function of the reduced frequency ( $k$ ), which is the non-dimensionalized oscillation rate of the airfoil. The reduced frequency may be regarded as a measure of the unsteadiness of the airflow. As the reduced frequency increases, the error inherent in quasi-steady 2-D aerodynamics becomes greater and greater, and the use of unsteady 2-D aerodynamics becomes increasingly significant in the calculation of an accurate flutter speed.

#### 3.6.5.1 Forming the Lagrange Equations of Motion using Unsteady Aerodynamic Forces and Moments

In unsteady flow, the reduced frequency of the section's oscillation is used to determine the effect that motion has on the lift force generated. As the airfoil section oscillates in the airstream, a changing trailing vortex is generated. This vortex acts in opposition to the circulation around the section. For example, when the section pitches nose up, the wake curls around the trailing edge in a direction opposite to the pitching motion. This reduces the lift force by reducing the circulation (Bisplinghoff, Ashley, 1962). Theodorsen's circulation function is a means of quantifying this wake-induced lift loss, where the values range from 1.0 to 0.5 as a function of the reduced frequency. In contrast, no reduction in lift force due to section oscillation occurs in quasi-steady flow, since the out-of-

phase component of lift force that results from the effects of the trailing vortices is, as we have seen in Section 3.6.4, omitted. Two basic approaches, both based on the determinant method for solving for the system's eigenvalues, are used to solve for the flutter frequency and speed when using unsteady 2-D aerodynamics.

#### 3.6.5.1.1 Finding the flutter frequency and speed – Theodorsen's Method

Theodorsen's method is based on the simultaneous solution of the real and imaginary parts of the flutter determinant. The flutter determinant arises from the same equations of motion used in the quasi-steady case, with the modification of the lift forces by the use of unsteady 2-D aerodynamics. The basic solution procedure is to choose a series of values of reduced frequency and find the corresponding roots of the real and imaginary characteristic equations. These roots, the eigenvalues of the system of equations of motion, are then plotted as functions of the reciprocal of the reduced frequency,  $(1/k)$ . The point on the graph where the two plots of the roots intersect is the point where the required condition of both the real and imaginary determinants equaling zero is simultaneously satisfied. Both the flutter frequency and the flutter speed are found at the intersection of the real and imaginary plots (Fung, 1969).

### 3.6.5.1.2 Finding the flutter frequency and speed – Materiel Center

#### Method

In Smilg and Wasserman's "Materiel Center" method, an artificial damping factor,  $g$ , (equal for both bending and torsional degrees of freedom) is introduced into the equations of motion. The attached Mathcad worksheets use this method, where the solution to the flutter frequency and speed is found when the artificial damping changes sign from negative to positive as a function of the reciprocal of the reduced frequency ( $1/k$ ). When the artificial damping factor is positive, the system is unstable, and therefore in a condition of flutter. This is due to the balance of forces needed to maintain system stability, as a positive artificial damping factor indicates a need for positive damping to be present in order to prevent instability. A negative artificial damping factor indicates a stable system, since there is, in its presence, an excess of damping available in the system. An artificial damping factor of zero implies the critical flutter condition (Donaldson, 1993).

The artificial damping factor is applied to the stiffness matrix, where it effectively supplements the system's resistance to deflection. It is inserted into the same equations of motion developed in Section 3.2, with the substitution of the lift and moment of unsteady aerodynamic forces. It

should be noted that in these equations, DOF  $h$  is oriented positive down (Smilg, Wasserman, 1942). The equations of motion for the case of unsteady 2-D aerodynamics are thus:

$$m \cdot \ddot{h} + m \cdot b \cdot \ddot{\alpha} + (1 + ig) \cdot k_b \cdot h = -L$$

$$m \cdot b \cdot \ddot{h} + H_{ea} \cdot \ddot{\alpha} + (1 + ig) \cdot K_T \cdot \alpha = M$$

The lift and moment expressions for unsteady 2-D aerodynamics are further discussed in Section 3.7.1.2. After rearranging to make the system of equation homogeneous, the equations of motion are thus:

$$m \cdot \ddot{h} + m \cdot b \cdot \ddot{\alpha} + (1 + ig) \cdot k_b \cdot h + L = 0$$

$$m \cdot b \cdot \ddot{h} + H_{ea} \cdot \ddot{\alpha} + (1 + ig) \cdot K_T \cdot \alpha - M = 0$$

### 3.7 Solution of the Double Eigenvalue Problem

Having derived the equations of motion, it is now necessary to solve the system of the equations of motion for its two eigenvalues. These are the values which cause the characteristic equation to equal zero, and are the squares of the flutter frequency and speed.

### 3.7.1 Placing the System in Simple Harmonic Motion

In both the quasi-steady and the unsteady 2-D aerodynamics case, the objective of the analysis is to locate the system's stability boundary, which is the airfoil section's critical flutter speed. This is determined by the critical speed of airflow at which the magnitudes of the bending and torsional oscillations are neither increasing nor decreasing. Since the neutral stability condition is to be tested, a logical approach is to insert solutions for simple harmonic motion into the equations of motion and then solve the system for the eigenvalues which will cause this condition to be satisfied. In the critical flutter condition, the bending and torsional motions, being constant in amplitude, are neither increasing nor decreasing, so it is appropriate to represent them as sinusoidal motions, as shown below, where  $A_1$ ,  $A_2$ , and  $B_1$  are the amplitudes of the torsional and bending motions, respectively. The motions of the two DOF are described by the sine function, and the cosine function provides a component with a 90-degree phase angle between the bending and torsional motions:

$$h(t) = B_1 \cdot \sin \omega t$$

$$\alpha(t) = A_1 \cdot \sin \omega t + A_2 \cdot \cos \omega t$$

To be clear on the matter of phase angles, note that if:

$$A_1 = A_0 \cdot \cos \phi$$

and

$$A_2 = A_0 \cdot \sin \phi$$

Then,

$$\alpha(t) = A_0 \cdot (\sin \omega t \cdot \cos \phi + \cos \omega t \cdot \sin \phi)$$

or

$$\alpha(t) = A_0 \cdot (\sin \omega t + \phi)$$

where  $\phi$  can be seen as the phase angle between bending and torsion.

Alternately, using complex notation, the multiplication of  $A_2$  by  $i$  also provides the 90-degree phase angle component between the bending and torsional motions:

$$h = B_1 \cdot e^{i\omega t}$$

$$\alpha = (A_1 + i \cdot A_2) \cdot e^{i\omega t}$$

Using the complex algebra form, and taking the first and second time derivatives of the two DOF:

$$\dot{h} = i \cdot \omega \cdot B_1 \cdot e^{i\omega t}$$

$$\ddot{h} = -\omega^2 \cdot B_1 \cdot e^{i\omega t}$$

$$\dot{\alpha} = i \cdot \omega (A_1 + i \cdot A_2) \cdot e^{i\omega t}$$

$$\ddot{\alpha} = -\omega^2 (A_1 + i \cdot A_2) \cdot e^{i\omega t}$$

Substituting these solutions into the equations of motion, canceling  $e^{i\omega t}$  for all terms, and casting in matrix form results in the matrix equations of motion. The solution to this system satisfies the condition of simple harmonic motion.

### 3.7.1.1 Flutter Solution in the case of Quasi-steady Aerodynamic Forces

Using the Equations of Motion derived in Section 3.2, forming the determinant, and separating into real and imaginary parts:

$$\left[ \begin{array}{c} \left( \begin{array}{cc} -m \cdot \omega^2 \cdot b - A_0 \cdot V^2 & k_b - m \cdot \omega^2 \\ K_T - H_{ea} \cdot \omega^2 - a \cdot A_0 \cdot V^2 & -m \omega^2 \cdot b \end{array} \right) \cdot \begin{pmatrix} A_1 \\ B_1 \end{pmatrix} \dots \\ + i \cdot \left[ \begin{array}{cc} \omega \cdot A_0 \cdot V & m \cdot \omega^2 \cdot b + A_0 \cdot V^2 \\ a \cdot \omega \cdot A_0 \cdot V & (K_T - H_{ea} \cdot \omega^2 - a \cdot A_0 \cdot V^2) \end{array} \right] \cdot \begin{pmatrix} B_1 \\ A_2 \end{pmatrix} \end{array} \right] = \begin{pmatrix} 0 \\ 0 \end{pmatrix}$$

It is now necessary to determine the eigenvalues of this system, that is, the frequency and velocity for which the required condition of both

the real and imaginary determinants equaling zero, is true. For this two DOF system, the determinant method is a convenient means of finding the eigenvalues. After expanding the complex determinant and solving the characteristic equation, the flutter frequency is:

$$\omega_f = \sqrt{\frac{K_T}{H_{ea} - m \cdot a \cdot b}}$$

Similarly, the real determinant yields the flutter speed:

$$V_f = \sqrt{\frac{\left(k_b - m \cdot \omega_f^2\right) \cdot \left(K_T - H_{ea} \cdot \omega_f^2\right) - \left(m \cdot b \cdot \omega_f^2\right)^2}{A_0 \cdot \left[a \cdot \left(k_b - m \cdot \omega_f^2\right) + m \cdot b \cdot \omega_f^2\right]}}$$

It should be noted here that when the CG is co-located with the EA, the lever arm distance (b) will be zero. In that case, the flutter frequency will be equal to the uncoupled torsional frequency, and the flutter speed will be zero. This result is compared with the flutter speed calculated by use of unsteady aerodynamics below, and illustrates a fundamental flaw in the use of quasi-steady aerodynamics.

### 3.7.1.2 Flutter Solution in the Case of Unsteady Aerodynamic Forces and Moments

The homogeneous equations of motion using the Material Center method were derived in Section 3.6.5.1.2. They are:

$$m \cdot \ddot{h} + m \cdot b \cdot \ddot{\alpha} + (1 + ig) \cdot k_b \cdot h + L = 0$$

$$m \cdot b \cdot \ddot{h} + H_{ea} \cdot \ddot{\alpha} + (1 + ig) \cdot K_T \cdot \alpha - M = 0$$

The lift force and the aerodynamic moment per unit span moment about the elastic axis resulting from the use of unsteady 2-D aerodynamics are functions of  $\ddot{h}, \dot{h}, \ddot{\alpha}, \alpha, V, \omega$ , and Theodorsen's circulation function,  $C(k)$  (Scanlon, Rosenbaum, 1968) :

$$L = \pi \cdot \rho b^3 \cdot \left[ \left( \frac{-\ddot{h}}{b'} - \frac{2 \cdot V}{b'} \cdot C(k) \cdot \frac{\dot{h}}{b'} + a_h \cdot \ddot{\alpha} \right) \dots \right. \\ \left. + \left[ 2 \cdot \left( a_h - \frac{1}{2} \right) \cdot (C(k) - 1) \right] \cdot \frac{V}{b'} \cdot \dot{\alpha} - \frac{2 \cdot V^2}{b'^2} \cdot C(k) \cdot \alpha \right]$$

$$M = \pi \cdot \rho b'^4 \cdot \left[ \begin{array}{l} \frac{a_h}{b'} \cdot \ddot{h} + \frac{2 \cdot \left( \frac{1}{2} + a_h \right)}{b'} \cdot C(k) \cdot \frac{V \cdot \dot{h}}{b'} - \left( \frac{1}{8} + a_h^2 \right) \cdot \ddot{\alpha} \dots \\ + \left[ \left[ a_h - \frac{1}{2} + 2 \cdot \left( \frac{1}{4} - a_h^2 \right) \cdot C(k) \right] \cdot \frac{V}{b'} \cdot \dot{\alpha} \dots \right. \\ \left. + 2 \cdot \left( \frac{1}{2} + a_h \right) \cdot C(k) \cdot \frac{V^2}{b'^2} \cdot \alpha \right] \end{array} \right]$$

Using the reduced frequency (k), Theodorsen's circulation function is calculated by use of Bessel Functions. The values for the lift and moment determined are then used to determine the values of the coefficients in the flutter determinant (Theodorsen, 1934).

$$F(k) = \frac{J_1(k) \cdot (J_1(k) + Y_0(k)) + Y_1(k) \cdot (Y_1(k) - J_0(k))}{(J_1(k) + Y_0(k))^2 + (Y_1(k) - J_0(k))^2}$$

$$G(k) = \frac{-Y_1(k) \cdot Y_0(k) - J_1(k) \cdot J_0(k)}{(J_1(k) + Y_0(k))^2 + (Y_1(k) - J_0(k))^2}$$

$$C(k) = F(k) + i \cdot G(k)$$

Again assuming harmonic motion, we use the substitutions of:

$$h = h_0 \cdot e^{i\omega t}$$

and

$\alpha = \alpha_0 \cdot e^{i\omega t}$  and their derivatives to replace the terms in the Lift and Moment equations, resulting in the equation of motion being stated in

terms of the non-dimensional DOF  $\frac{h}{b'}$  and  $\alpha$ . The lift and moment coefficients for bending and torsion are functions of the reduced frequency (Kussner, Schwartz, 1935):

$$L_h(k) = 1 - 2 \cdot i \cdot \left( \frac{1}{k} \right) \cdot C(k)$$

$$L_\alpha(k) = \frac{1}{2} - i \cdot \left( \frac{1}{k} \right) \cdot (1 + 2 \cdot C(k)) - 2 \cdot \left( \frac{1}{k} \right)^2 \cdot C(k)$$

$$M_h = \frac{1}{2}$$

$$M_\alpha(k) = \frac{3}{8} - i \cdot \left( \frac{1}{k} \right)$$

In these equations,  $L_h$ ,  $L_\alpha$ , and  $M_\alpha$  are the lift and aerodynamic moment coefficients about the elastic axis as functions of the reduced frequency, while  $M_h$  is a constant,  $\frac{1}{2}$ . These values are also substituted into the equations of motion:

$$\bar{L} = -\pi \rho b'^3 \omega^2 \cdot \left[ L_h \cdot \frac{h}{b'} + \left[ L_\alpha - \left( \frac{1}{2} + a_h \right) \cdot L_h \right] \cdot \alpha \right]$$

$$M = \pi \cdot \rho b'^4 \cdot \omega^2 \cdot \left[ \left[ \left( M_h - \left( \frac{1}{2} + a_h \right) \cdot L_h \right) \cdot \frac{h}{b'} \dots \right] + \left[ M_\alpha - \left( \frac{1}{2} + a_h \right) \cdot (L_\alpha + M_h) \dots \right] \cdot \alpha \right]$$

Dividing out  $\pi \cdot \rho b'^3 \cdot \omega^2$  from the bending equation, and  $\pi \cdot \rho b'^4 \cdot \omega^2$  from the torsional equation to express the Lift and Moment coefficients in non-dimensional form:

$$L = - \left[ L_h \cdot \frac{h}{b'} + \left[ L_\alpha - \left( \frac{1}{2} + a_h \right) \cdot L_h \right] \cdot \alpha \right]$$

$$M = \left[ M_h - \left( \frac{1}{2} + a_h \right) \cdot L_h \right] \cdot \frac{h}{b'} \dots + \left[ M_\alpha - \left( \frac{1}{2} + a_h \right) \cdot (L_\alpha + M_h) + \left( \frac{1}{2} + a_h \right)^2 \cdot L_h \right] \cdot \alpha$$

Defining the complex variable Z:

$$Z = \left( \frac{\omega_T}{\omega} \right)^2 \cdot (1 + i \cdot g) \quad (\text{Smilg, Wasserman, 1942}).$$

and substituting into the equations of motion, after transposing, results in:

$$\begin{bmatrix} \mu \cdot \left[ 1 - Z \cdot \left( \frac{\omega_b}{\omega_T} \right)^2 \cdot (1 + i \cdot g) \right] \cdot L_h(k) \cdot \frac{h}{b'} \dots \\ + \left[ \mu \cdot x_\alpha + L_\alpha(k) - L_h(k) \cdot \left( \frac{1}{2} + a_h \right) \right] \cdot \alpha \end{bmatrix} = 0$$

$$\begin{bmatrix} \left[ \mu \cdot x_\alpha + M_h - L_h(k) \cdot \left( \frac{1}{2} + a_h \right) \right] \cdot \frac{h}{b'} \dots \\ + \left[ \mu \cdot r_\alpha^2 [1 - X \cdot (1 + i \cdot g)] - \frac{1}{2} \cdot \left( \frac{1}{2} + a_h \right) \dots \right. \\ \left. + M_\alpha(k) - L_\alpha(k) \cdot \left( \frac{1}{2} + a_h \right) + L_h(k) \cdot \left( \frac{1}{2} + a_h \right)^2 \right] \cdot \alpha \end{bmatrix} = 0$$

Casting the system of equations of motion in matrix form,

$$\begin{bmatrix} \mu \cdot \left[ 1 - Z \cdot \left( \frac{\omega_b}{\omega_T} \right)^2 \cdot (1 + i \cdot g) \right] \cdot L_h(k) & \mu \cdot x_\alpha + L_\alpha(k) - L_h(k) \cdot \left( \frac{1}{2} + a_h \right) \\ \mu \cdot x_\alpha + M_h - L_h(k) \cdot \left( \frac{1}{2} + a_h \right) & \mu \cdot r_\alpha^2 [1 - X \cdot (1 + i \cdot g)] - \frac{1}{2} \cdot \left( \frac{1}{2} + a_h \right) \dots \\ & + M_\alpha(k) - L_\alpha(k) \cdot \left( \frac{1}{2} + a_h \right) + L_h(k) \cdot \left( \frac{1}{2} + a_h \right)^2 \end{bmatrix} \cdot \begin{pmatrix} \frac{h}{b'} \\ \alpha \end{pmatrix} = 0$$

Setting the determinant equal to zero,

$$\begin{vmatrix} \mu \left[ 1 - Z \cdot \left( \frac{\omega_b}{\omega_T} \right)^2 \cdot (1 + i \cdot g) \right] \cdot L_h(k) & \mu \cdot x_\alpha + L_\alpha(k) - L_h(k) \cdot \left( \frac{1}{2} + a_h \right) \\ \mu \cdot x_\alpha + M_h - L_h(k) \cdot \left( \frac{1}{2} + a_h \right) & \mu \cdot r_\alpha^2 \cdot [1 - X \cdot (1 + i \cdot g)] - \frac{1}{2} \cdot \left( \frac{1}{2} + a_h \right) \dots \\ & + M_\alpha(k) - L_\alpha(k) \cdot \left( \frac{1}{2} + a_h \right) + L_h(k) \cdot \left( \frac{1}{2} + a_h \right)^2 \end{vmatrix} = 0$$

The flutter determinant elements may be simplified by using the following substitutions (A, B, D & E):

$$A = \mu \cdot \left[ 1 - Z \cdot \left( \frac{\omega_b}{\omega_T} \right)^2 \cdot (1 + i \cdot g) \right] \cdot L_h(k)$$

$$B = \mu \cdot x_\alpha + L_\alpha(k) - L_h(k) \cdot \left( \frac{1}{2} + a_h \right)$$

$$D = \mu \cdot x_\alpha + M_h - L_h(k) \cdot \left( \frac{1}{2} + a_h \right)$$

$$E = \mu \cdot r_\alpha^2 [1 - X \cdot (1 + i \cdot g)] - \frac{1}{2} \cdot \left( \frac{1}{2} + a_h \right) + M_\alpha(k) - L_\alpha(k) \cdot \left( \frac{1}{2} + a_h \right) \dots \\ + L_h(k) \cdot \left( \frac{1}{2} + a_h \right)^2$$

The equations of motion, in terms of the above, are thus:

$$A \cdot \frac{h}{b'} + B\alpha = 0$$

$$D \cdot \frac{h}{b'} + E\alpha = 0$$

Casting in matrix form:

$$\begin{pmatrix} A & B \\ D & E \end{pmatrix} \cdot \begin{pmatrix} \frac{h}{b'} \\ \alpha \end{pmatrix} = 0$$

Setting the determinant of the system to zero:

$$\left| \begin{pmatrix} A & B \\ D & E \end{pmatrix} \right| = 0$$

The characteristic equation, including the real and imaginary values, is thus:

$$A \cdot E - B \cdot D = 0$$

The Mathcad worksheet calculates the values of the determinant elements A, B, D and E instead of using the tabular values found in

USAAF Technical Report 4798. The complex characteristic equation is then formed, and the Polyroots function of Mathcad is used to determine the real and complex roots of the resulting quadratic equation. The lesser of these two roots, which represents the unstable torsional motion, will always contain the imaginary component which changes sign from negative to positive as the reciprocal of the reduced frequency increases (Bisplinghoff, Ashley, and Halfman, 1955).

Since  $\omega$  and  $g$  always appear together in the determinantal elements A and E, by solving for Z, both  $\omega$  and  $g$  can be determined. Representing the unstable torsional motion, the first root of Z, as a function of reduced frequency ( $k$ ),  $Z(k)_1$ , is used in the calculation of the artificial damping. The system damping is determined by taking the ratio of the imaginary part to the real part of the first root of the frequency quadratic. When the sign of  $g$  changes from negative to positive as a function of the sign of  $Z(k)_1$ , instability is indicated, where a positive  $g$  indicates flutter:

$$g_{\text{art}} = \frac{\text{Im}(Z(k)_1)}{\text{Re}(Z(k)_1)}$$

Since

$X = \left( \frac{\omega_T}{\omega} \right)^2$ , and X is the real part of Z, the flutter frequency is found using the uncoupled torsional frequency and the real part of the first root of the characteristic equation:

$$\omega_{fl} = \frac{\omega_T}{\sqrt{\text{Re}(Z(k)_1)}}$$

The flutter speed is then found by using the flutter frequency, the section semi-span, and the reduced frequency, using the relation:

$$V_{fl} = \frac{\omega_{fl} \cdot b'}{k}$$

Using the Materiel Center method, the goal is to find the airspeed that causes the artificial damping factor to go from negative artificial damping (stability) to zero (criticality), the point of neutral stability, and thus determine the critical flutter speed. This is accomplished by varying the reciprocal of the reduced frequency ( $1/k$ ) over a suitable range and solving the system for the value of the artificial damping. The value of the reciprocal of the reduced frequency that causes the artificial damping to go from negative to zero is then used to calculate the flutter frequency and velocity. The values of artificial damping ( $g$ ) versus reduced frequency

may be plotted to observe the trend in damping as the reduced frequency is increased. This is illustrated in Figure 3.7.1.2.1.

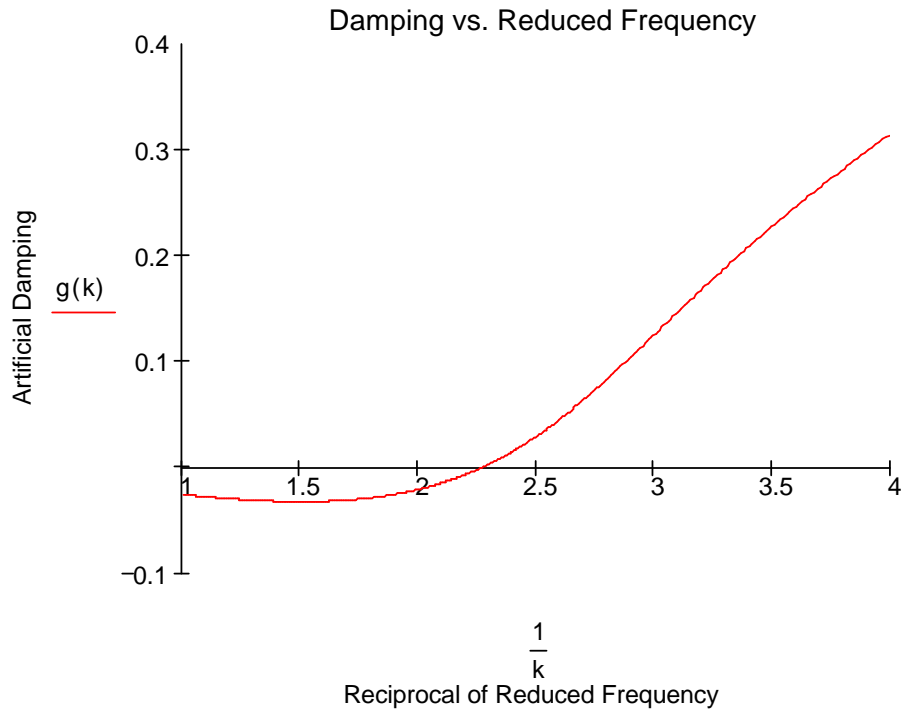


Figure 3.7.1.2.1 Artificial damping versus reduced frequency

The slope of the damping curve gives an indication of the severity of the onset of flutter in that the rate of the instability may be predicted. A shallow slope indicates a less severe onset of flutter, whereas a steep slope implies that a violent encounter with flutter may be expected (Bisplinghoff, Ashley, and Halfman, 1955). The attached Mathcad worksheets carry out these calculations as a result of the input variables

provided. Figure 3.7.1.2.2 depicts the artificial damping versus the speed of the airflow in knots.

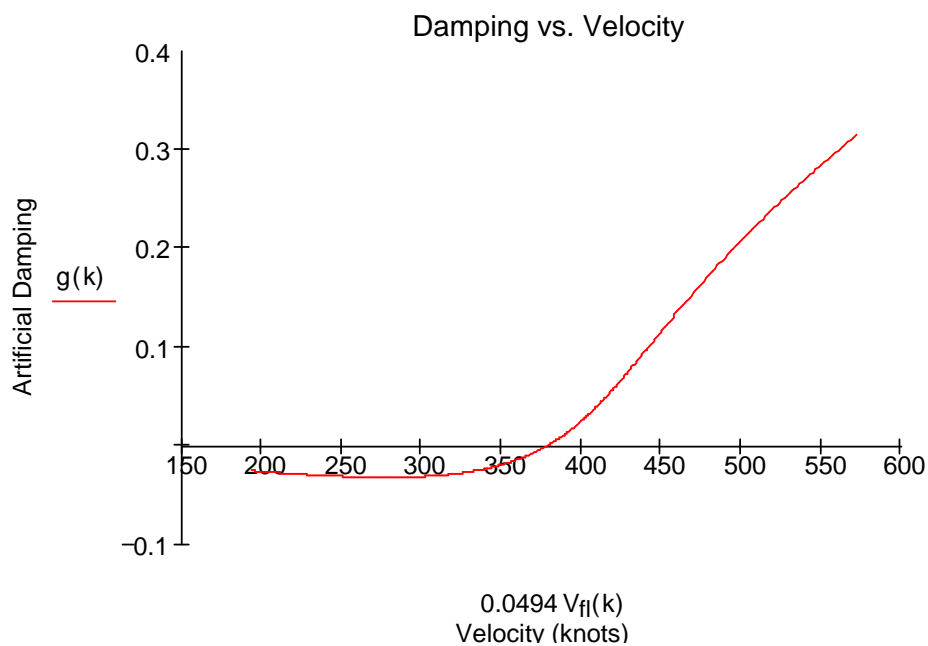


Figure 3.7.1.2.2 Artificial damping versus velocity

### 3.8 Chapter Summary

The basic means of establishing the equations of motion is the same in both the quasi-steady and the unsteady cases. Using Lagrange's equation and the appropriate expressions for (1) the strain energy, (2) the kinetic energy, and (3) the aerodynamic forces leads to the homogeneous equations of motion. The two descriptions of the aerodynamic forces considered here are quasi-steady and unsteady 2-D aerodynamic forces

and moments. Both the quasi-steady and unsteady 2-D cases use the determinant method to establish the characteristic equation, which is then solved for its roots. Accuracy is improved by the use of the unsteady aerodynamic forces and moments, while the quasi-steady solution method, within its range of validity with respect to CG position, is more rapidly solved and results in a conservative calculation (Bisplinghoff, Ashley, and Halfman, 1955).

## **Chapter 4.0: Calculation of Flutter Properties by Mathcad**

### **Worksheets**

This section describes the calculation methodology used in the attached Mathcad worksheet to determine the flutter frequency and the critical flutter speed of six example sections. Using both quasi-steady and unsteady aerodynamics, flutter properties of the example sections are calculated in the worksheet using a common set of section parameters. The objective is to input the key structural and inertial parameters that affect the value of the flutter frequency and speed and compare the section's flutter properties using quasi-steady and unsteady aerodynamic forces. For the case of center of gravity (CG) variation, results are plotted for both cases and compared. An example of flutter speed variation with altitude is also performed in one example.

#### **4.1 Mathcad Worksheet Methodology**

The Mathcad Worksheet processing flow follows the pattern of inputs, intermediate or supporting calculations, and outputs. The means by which each of these is carried is as follows.

#### 4.1.1 Program inputs

User inputs (the boxed quantities on the worksheet) define the primary airfoil section elastic, inertial and aerodynamic parameters common to both the quasi-steady and unsteady cases. The basic section parameters of section chord, section aerodynamic center, center of gravity and elastic axis location, the section weight per inch of span length ( $Wt$ ), the section mass moment of inertia about the center of gravity per inch ( $H_{cg}$ ), and the section bending and torsional stiffnesses per inch are input. For the quasi-steady calculation, the section lift curve slope for a given airfoil ( $C_{l\alpha}$ ), drawn from Table 3.6.3, and the strip width ( $w$ , an arbitrary value) are also inputs. Additionally, the air properties are included as inputs, such as the International Standard Atmosphere (ISA) air density ( $\rho$ ) and the density ratio ( $\delta$ ) as required for test altitude. The user may vary any input as desired to test for flutter frequency and speed sensitivity with respect to that particular parameter or any combination of input parameters.

#### 4.1.2 Supporting calculations

The worksheet prepares intermediate calculations for use in both the quasi-steady and unsteady cases. The lever arm distances from the section aerodynamic center to the elastic axis ( $a$ ), and from the section elastic axis to the center of gravity ( $b$ ), the section mass ( $m$ ), and the section mass moment of inertia about the elastic axis ( $H_{ea}$ ) are calculated for internal program use. The air density ratio as a function of altitude and the air density at test condition are provided to allow test altitudes above Sea Level.

##### 4.1.2.1 Quasi-steady Case

For the quasi-steady case, the strip properties of strip area, stiffness and mass moment of inertia are calculated. These are used to define the elastic, inertial and aerodynamic forces arising from any given strip width.

##### 4.1.2.2 Unsteady Case

For the unsteady case, several additional non-dimensional quantities are derived from the basic program inputs. These include the

section semi-chord ( $b$ ), the uncoupled bending and torsional natural frequencies ( $\omega_b$ ,  $\omega_T$ ), the dimensionless center of gravity ( $x_\alpha$ ) and elastic axis positions ( $a_h$ ), the dimensionless radius of gyration ( $r_\alpha$ ) and the section mass ratio ( $\mu$ ). Many of the references cited in this thesis use the uncoupled bending-torsional natural frequency ratio to define the section properties. It is thus calculated in order to cross check these values with the section input parameters. The section static imbalance,  $S_\alpha$ , similarly provides an input cross-check. As these quantities are often presented in the literature in this non-dimensional form, this feature allows convenient comparison of dimensional and non-dimensional inputs, as applicable. It also allows direct entry of all non-dimensional parameters, if desired.

A final supporting calculation useful for both cases is the check of the section static divergence speed ( $V_D$ ). This value provides an upper limit on the range of flutter speeds to be evaluated, as any flutter speed calculated above this value would be unattainable, since the section would have failed in static divergence prior to experiencing flutter.

### 4.1.3 Primary calculations

#### 4.1.3.1 Quasi-steady Case

The flutter frequency and speed are found by direct calculation of the closed form equations of Section 3.7.1.1. For the CG variation study, the CG position is varied from the aerodynamic center location at the quarter chord to the trailing edge of the airfoil and plotted.

#### 4.1.3.2 Unsteady Case

For the unsteady flutter calculation, the program uses an initial value of the reduced frequency ( $k$ ). It calculates the value of Theodorsen's function,  $C(k)$ , and the unsteady lift and moments due to section bending and torsion. The determinant elements are then calculated and the resulting characteristic quadratic equation solved for its roots using the Polyroots root finder function of Mathcad. This process is carried out for a series of reciprocals of the reduced frequency until the program finds the reciprocal of the reduced frequency ( $1/k$ ) that causes the artificial damping ( $g$ ) to become zero. These values are plotted to show the trend of damping versus the reciprocal of the reduced frequency. A similar calculation loop is carried out to find the flutter frequency and

speed, both graphically and numerically. A plot of damping versus velocity of airflow then is used to depict the artificial damping and also the flutter speed.

CG variation is again accomplished by the use of the same program operating on a series of CG change increments. The results of the flutter speed as a function of CG position is plotted.

#### 4.1.4 Program Outputs

The program outputs are shown as the boxed and shaded quantities on the Mathcad worksheet. The quasi-steady flutter frequency and speed are the imaginary and real eigenvalues of the system of the equations of motion of the section. Unsteady case program outputs (all functions of reduced frequency) are the artificial damping ( $g$ ), the phase angle at zero artificial damping ( $\phi$ ), the flutter frequency ( $\omega_{fl}$ ), and the critical flutter speed ( $V_{fl}$ ).

## 4.2 Example Calculations

The following six airfoil sections were evaluated using the Mathcad worksheet to determine their flutter characteristics. The sources for these sections range from published technical reports and textbooks to information located on the Internet in the case of a newly-designed aircraft. In all cases, a check of the static divergence speed confirmed that all sections would experience flutter at speeds below the divergence speed.

#### 4.2.1 Example One: Ryan NYP prototype (Blevins, 1990)

##### 4.2.1.1 Inputs, Intermediate Calculations and Outputs

###### Program Inputs

Section Chord	84	Inch
Strip Width	10	Inch
AC location	0.25	Tenths of chord
CG Location	0.4	Tenths of chord
EA Location	0.26	Tenths of chord
Section Bending Stiffness	12.25	Pounds per Inch
Section Torsional Stiffness	6084	Inch-Pounds per Radian
Section Weight per unit span	0.81	Pounds per Inch
Section Mass Moment of Inertia about CG	8.75	Slug-inch <sup>2</sup> per inch
Air Density at ISA conditions	0.002378	Slugs/cubic foot
Test Altitude	0 (Sea Level)	Feet
Airfoil Lift Curve Slope	0.084	Per degree

###### Intermediate Calculations

Air Density Ratio at Test Condition	1.0	Non Dimensional
Uncoupled Natural Bending Frequency	22.1	Radians/Sec
Uncoupled Natural Torsional Frequency	22.3	Radians/Sec
CG Position	0.28	Non Dimensional
EA Position	-0.48	Non Dimensional
Section Static Imbalance	0.296	Slug-inch
Radius of Gyration	0.525	Non Dimensional
Mass ratio	3.3	Non Dimensional

Static Divergence Speed	252.1	Knots
Program Outputs		
Quasi-steady (QS) Flutter Frequency	22.08	Radians/Sec
Quasi-steady (QS) Flutter Speed	35.6	Knots
Reduced Frequency (k) at Zero Damping	1.0	Non Dimensional
Unsteady (US) Flutter Frequency	27.32	Radians/Sec
Unsteady (US) Flutter Speed	53.5	Knots
Ratio of QS to US flutter frequency	0.81	Non Dimensional
Ratio of QS to US flutter speed	0.63	Non Dimensional

#### 4.2.1.2 Section Characteristics

This wing section is the preliminary design of wood and fabric construction for the single-engine, special-purpose aircraft, "The Spirit of St. Louis". It is typical of the design and construction methodology of the late 1920's. The braced wing section is composed of two main spars, both made of wood, with a covering of doped fabric which acts as the non-load bearing skin. The parameters listed are found on pages 141-144 of Reference Nine. The section is exceptionally light, with the mass ratio of 3.3 being the lowest of all sections tested. A low mass ratio typically

indicates a low flutter speed due to the high propensity for the section to experience flow-induced vibration. The torsional natural frequency is the lowest of all the example sections. Also, little frequency separation between the natural bending and torsional frequencies is present, suggesting the possibility of a low flutter speed. Finally, the section has the most aft CG of all the sections.

#### 4.2.1.3. Flutter Calculations for the Quasi-steady Case

The flutter frequency of 22.08 Rad/sec is approximately equal to the natural bending frequency. The flutter speed of 35.6 knots is within 4% of that published in Reference Nine of 37.0 knots.

#### 4.2.1.4 Flutter Calculations for the Unsteady Case

The reduced frequency at zero damping is found to be 1.0. This indicates a relatively slow rate of section oscillation. Notably, the coupled flutter frequency of 27.14 Rad/sec is greater than both the natural bending and torsional frequencies. This is unusual, but not unheard of (Bisplinghoff, Ashley, and Halfman, 1955). The critical flutter speed of 56.3 knots falls short of the design requirement of 112 knots. In this case, it is necessary to make changes in the section torsional stiffness and /or

the CG position to increase the critical flutter speed.

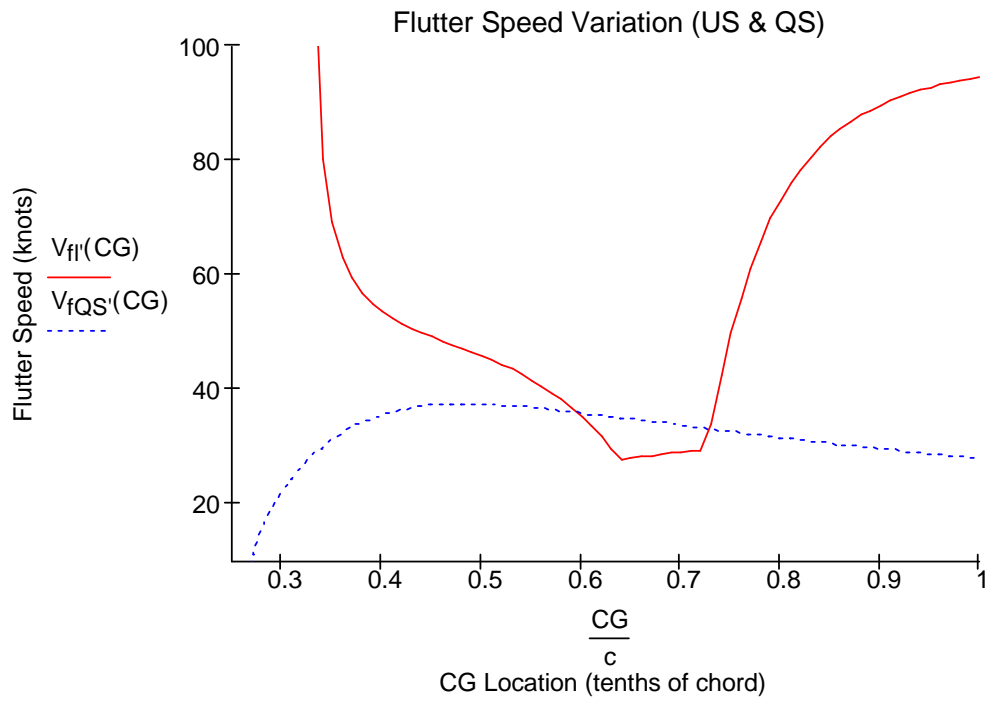
The low flutter speed found in this example shows how flutter may occur at low speeds. A common misconception is that if an aircraft is “slow”, it will not be subject to the effects of flutter. This is seen to be false, as the combination of the elastic, inertial and aerodynamic forces are responsible for flutter occurrence, and not merely the range of airspeed values attainable.

#### 4.2.1.5 Comparison of Results in the Quasi-steady and Unsteady Cases

The quasi-steady flutter frequency is 81% of the unsteady flutter frequency, while the quasi-steady flutter speed is 63% of the unsteady flutter speed. These are typical values for this comparison (Bisplinghoff, Ashley, and Halfman, 1955).

#### 4.2.1.6 CG Variation Survey

The sharp decrease in the critical flutter speed indicates a great sensitivity to CG position. Also, at the design condition of CG at  $0.4c$ , the flutter speed using quasi-steady aerodynamics is seen. The two speeds are equal at a CG position of about  $0.6c$ .



#### 4.2.2 Example Two: Ryan NYP Final Design (Blevins, 1990)

##### 4.2.2.1 Inputs, Intermediate Calculations and Outputs

###### **Program Inputs**

Section Chord	84	Inch
Strip Width	10	Inch
AC location	0.25	Tenths of chord
CG Location	0.4	Tenths of chord
EA Location	0.26	Tenths of chord
Section Bending Stiffness	49	Pounds per Inch
Section Torsional Stiffness	24336	Inch-Pounds per Radian
Section Weight per unit span	0.81	Pounds per Inch
Section Mass Moment of Inertia about CG	8.75	Slug-inch <sup>2</sup> per inch
Air Density at ISA conditions	0.002378	Slugs/cubic foot
Test Altitude	0 (Sea Level)	Feet
Airfoil Lift Curve Slope	0.084	Per degree

###### **Intermediate Calculations**

Air Density Ratio at Test Condition	1.0	Non Dimensional
Uncoupled Natural Bending Frequency	44.14	Radians/Sec
Uncoupled Natural Torsional Frequency	44.61	Radians/Sec
CG Position	0.28	Non Dimensional
EA Position	-0.48	Non Dimensional
Section Static Imbalance	0.296	Slug-inch
Radius of Gyration	0.525	Non Dimensional
Mass ratio	3.3	Non Dimensional
Static Divergence Speed	504.1	Knots

### **Program Outputs**

Quasi-steady (QS) Flutter Frequency	44.16	Radians/Sec
Quasi-steady (QS) Flutter Speed	71.1	Knots
Reduced Frequency (k) at Zero Damping	1.06	Non Dimensional
Unsteady (US) Flutter Frequency	54.64	Radians/Sec
Unsteady (US) Flutter Speed	107.1	Knots
Ratio of QS to US flutter frequency	0.81	Non Dimensional
Ratio of QS to US flutter speed	0.66	Non Dimensional

#### 4.2.2.2 Section Characteristics

In this case, the same input parameters given in Example One are repeated, with the design modification of the bending and torsional stiffnesses. These have been quadrupled by the addition of four external wing struts in order to meet the design requirement of a maximum speed of 107 knots, as described in Reference Nine.

#### 4.2.2.3 Flutter Calculations for the Quasi-steady Case

The flutter frequency of 44.16 rad/sec is twice that found in

Example One, as a result of the quadrupled stiffnesses. This value remains approximately equal to the natural bending frequency. The flutter speed of 107 knots is also twice that found in Example One.

#### 4.2.2.4 Flutter Calculations for the Unsteady Case

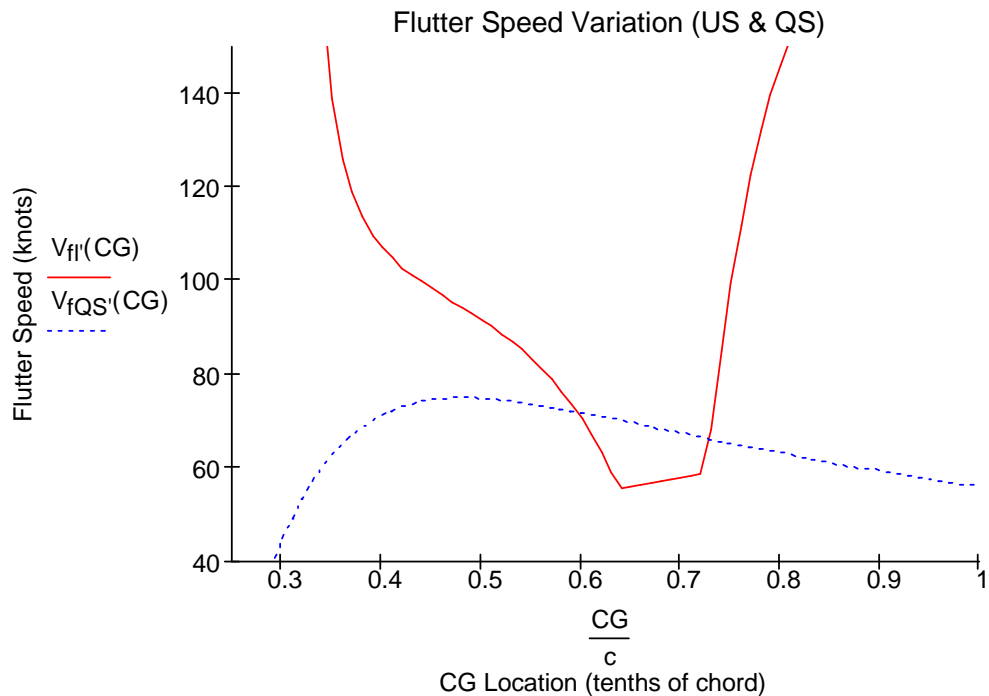
The reduced frequency for zero artificial damping in the unsteady case is 1.06. The unsteady flutter frequency remains greater than both the natural bending and torsional frequencies at 54.64 rad /sec. The flutter speed of 107 knots now meets the design requirement of 120 miles per hour as a result of the quadrupled stiffnesses. These results may be generalized to conclude that flutter speed increases as the square root of the stiffness.

#### 4.2.2.5 Comparison of Results in the Quasi-steady and Unsteady Cases.

The quasi-steady flutter frequency is 81% of unsteady flutter frequency, while the quasi-steady flutter speed is 63% of the unsteady flutter speed. This is identical to the results found in the prototype (Example 1) despite the quadrupled bending and torsional stiffnesses.

#### 4.2.2.6 CG Variation Survey

The increased flutter speeds for all CG positions is noted. Again the quasi-steady and unsteady flutter speeds are equal at about 0.6c.



#### 4.2.3 Example Three: MD3-160 Aircraft Section (Usmani, Ho, 2003)

##### 4.2.3.1 Inputs, Intermediate Calculations and Outputs

###### **Program Inputs**

Section Chord	60	Inch
Strip Width	10	Inch
AC location	0.25	Tenths of chord
CG Location	0.5	Tenths of chord
EA Location	0.4	Tenths of chord
Section Bending Stiffness	114	Pounds per Inch
Section Torsional Stiffness	132756	Inch-Pounds per Radian
Section Weight per unit span	0.83	Pounds per Inch
Section Mass Moment of Inertia about CG	13.74	Slug-inch <sup>2</sup> per inch
Air Density at ISA conditions	0.002378	Slugs/cubic foot
Test Altitude	0 (Sea Level)	Feet
Airfoil Lift Curve Slope	0.104	Per degree

###### **Intermediate Calculations**

Air Density Ratio at Test Condition	1.0	Non Dimensional
Uncoupled Natural Bending Frequency	66.5	Radians/Sec
Uncoupled Natural Torsional Frequency	95.14	Radians/Sec
CG Position	0.2	Non Dimensional
EA Position	-0.2	Non Dimensional
Section Static Imbalance	0.155	Slug-inch
Radius of Gyration	0.7952	Non Dimensional
Mass ratio	6.62	Non Dimensional
Static Divergence Speed	382.5	Knots

### **Program Outputs**

Quasi-steady (QS) Flutter Frequency	90.92	Radians/Sec
Quasi-steady (QS) Flutter Speed	112.6	Knots
Reduced Frequency (k) at Zero Damping	0.85	Non Dimensional
Unsteady (US) Flutter Frequency	91.34	Radians/Sec
Unsteady (US) Flutter Speed	159.3	Knots
Ratio of QS to US flutter frequency	1.00	Non Dimensional
Ratio of QS to US flutter speed	0.71	Non Dimensional

#### 4.2.3.2 Section Characteristics

This section is from a light two-place, single-engine sport and training aircraft. It uses an all-aluminum, semi-monocoque (stressed skin, load bearing) cantilever wing design. This section is the least statically imbalanced of all the sections tested, while the radius of gyration is the highest. The CG position for the test case is located fairly far aft at 0.5c. In addition to the CG study, this section is used to carry out an altitude variation study. The increase in the critical flutter speed as test altitude is increased is determined and plotted.

#### 4.2.3.3 Flutter Calculations for the Quasi-steady Case

The flutter frequency 90.92 Rad/sec, falling between the bending and torsional uncoupled natural frequencies as expected. The flutter speed is 112.6 knots.

#### 4.2.3.4 Flutter Calculations for the Unsteady Case

The reduced frequency for zero artificial damping in the unsteady case is 0.9. The flutter frequency is 91.34 rad/sec, and the flutter speed is calculated at 159.3 knots.

#### 4.2.3.5 Comparison of Results in the Quasi-steady and Unsteady Cases

The quasi-steady flutter frequency is 100% of the unsteady flutter frequency, while the quasi-steady flutter speed is 71% of the unsteady flutter speed. This was the closest conformance of quasi-steady to unsteady flutter speed calculations of all six examples.

The design criteria stated in Reference 15 was for freedom from flutter for airspeeds up to 120 knots. These results indicate that design target has been achieved. Flight testing would be required to verify these calculations.

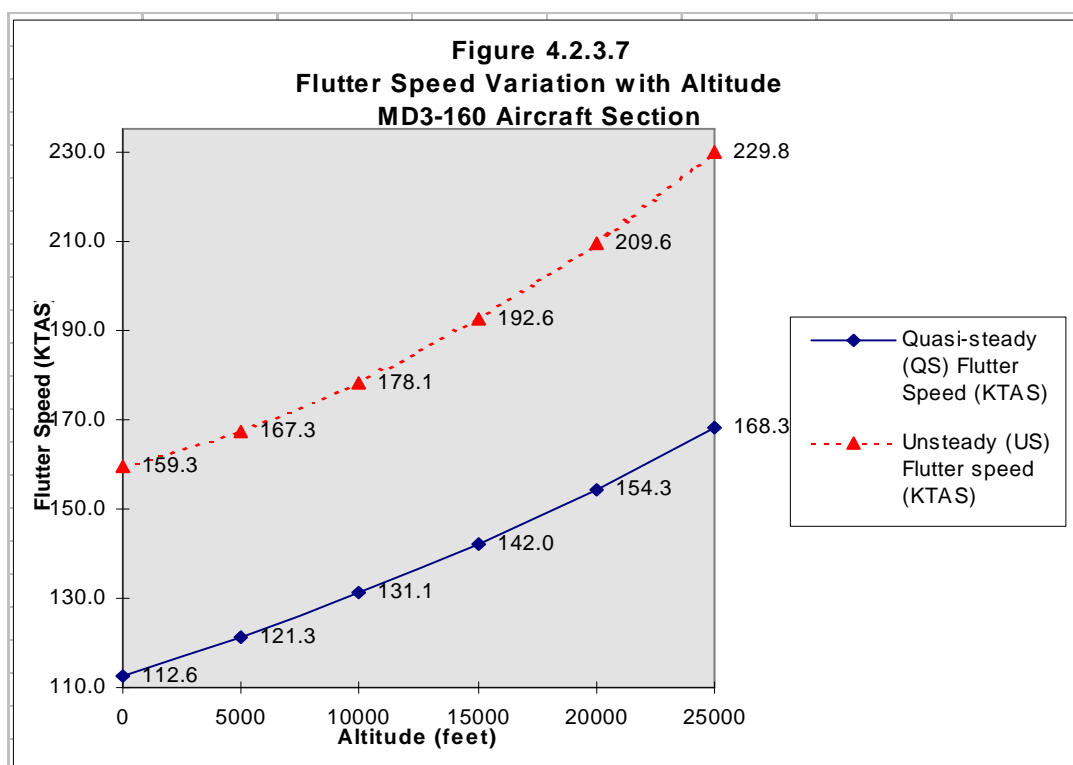
#### 4.2.3.6 Altitude Variation Survey

The increase in flutter speed predicted in Section 3.6.1 is demonstrated in Table 4.2.3 7 and Figure 4.2.3 7. Both the quasi-steady and unsteady flutter speeds (as true airspeeds) increase as altitude increases from Sea Level to 25,000 feet. The quasi-steady flutter speed remains approximately 71% of the unsteady flutter speed throughout this altitude range.

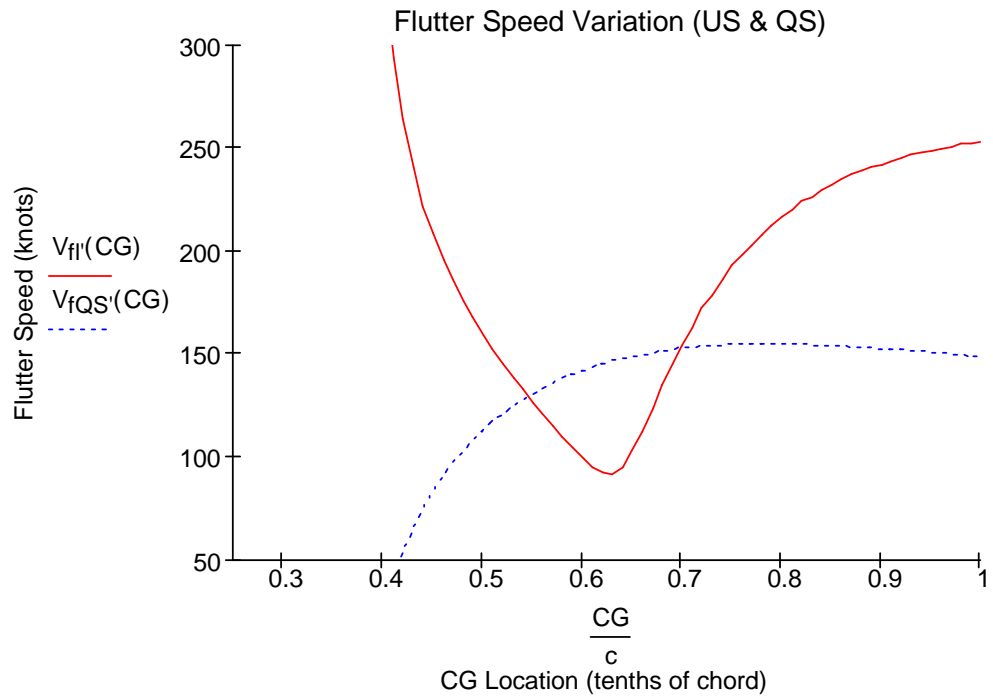
**Table 4.2.3.7**

**Flutter Speed Variation with Altitude**

<b>Test Altitude (feet)</b>	<b>Quasi-steady (QS) Flutter Speed (KTAS)</b>	<b>Unsteady (US) Flutter speed (KTAS)</b>	<b>QS/US Speed Ratio</b>	<b>Unsteady (US) Flutter speed (KIAS)</b>
0	112.6	159.3	0.71	159.3
5000	121.3	167.3	0.73	155.3
10000	131.1	178.1	0.74	153.0
15000	142.0	192.6	0.74	152.8
20000	154.3	209.6	0.74	153.0
25000	168.3	229.8	0.73	153.8



#### 4.2.3.7 CG Variation Survey



4.2.4 Example Four: Example from NACA Technical Report 685,  
(Theodorsen, Garrick, 1938)

4.2.4.1 Inputs, Intermediate Calculations and Outputs

**Program Inputs**

Section Chord	144	Inch
Strip Width	10	Inch
AC location	0.25	Tenths of chord
CG Location	0.4	Tenths of chord
EA Location	0.3	Tenths of chord
Section Bending Stiffness	45.4	Pounds per Inch
Section Torsional Stiffness	948572	Inch-Pounds per Radian
Section Weight per unit span	2.9	Pounds per Inch
Section Mass Moment of Inertia about CG	97.6	Slug-inch <sup>2</sup> per inch
Air Density at ISA conditions	0.002378	Slugs/cubic foot
Test Altitude	0 (Sea Level)	Feet
Airfoil Lift Curve Slope	0.104	Per degree

**Intermediate Calculations**

Air Density Ratio at Test Condition	1.0	Non Dimensional
Uncoupled Natural Bending Frequency	22.45	Radians/Sec
Uncoupled Natural Torsional Frequency	90.32	Radians/Sec
CG Position	0.2	Non Dimensional
EA Position	-0.4	Non Dimensional
Section Static Imbalance	1.297	Slug-inch
Radius of Gyration	0.499	Non Dimensional

Mass ratio	4.02	Non Dimensional
Static Divergence Speed	737.9	Knots

**Program Outputs**

Quasi-steady (QS) Flutter Frequency	86.9	Radians/Sec
Quasi-steady (QS) Flutter Speed	201.2	Knots
Reduced Frequency (k) at Zero Damping	0.4	Non Dimensional
Unsteady (US) Flutter Frequency	56.32	Radians/Sec
Unsteady (US) Flutter Speed	500.8	Knots
Ratio of QS to US flutter frequency	1.54	Non Dimensional
Ratio of QS to US flutter speed	0.40	Non Dimensional

4.2.4.2 Section Characteristics

The section characteristics are taken from the subject NACA report. The type of aircraft and its construction is unknown. Notably, the section had the broadest chord and the highest torsional stiffness in the series, although not the highest natural torsional frequency.

#### 4.2.4.3 Flutter Calculations for the Quasi-steady Case

The flutter frequency is 86.9 Rad/sec, coalescing between the bending and torsional uncoupled natural frequencies. The flutter speed is calculated at 201.2 knots.

#### 4.2.4.4 Flutter Calculations for the Unsteady Case

In contrast to previous examples, a significantly lower reduced frequency ( $k$ ) at zero artificial damping is found for this airfoil section. The reduced frequency is found to be 0.4 at zero artificial damping.

The unsteady flutter frequency is greater than both the natural bending and torsional frequencies at 56.32 rad/sec. The flutter speed is 500.8 knots, well into the compressible range and above the valid range of incompressible speeds for which this methodology is intended. Corrections for compressibility would be required.

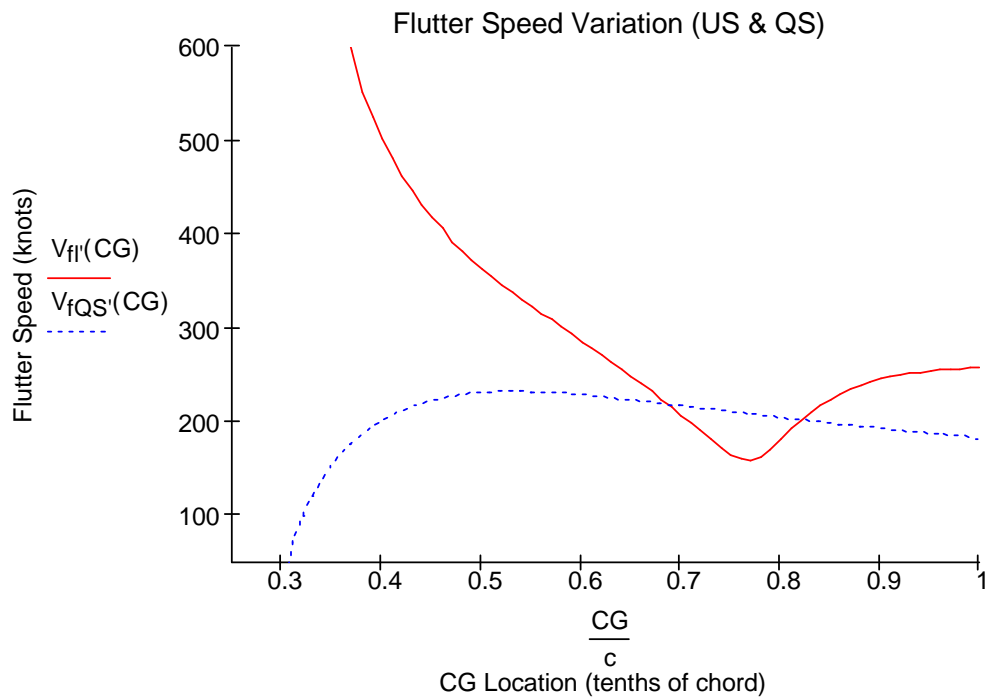
#### 4.2.4.5 Comparison of Results in the Quasi-steady and Unsteady Cases

The quasi-steady flutter frequency is 154% of the unsteady flutter frequency, while the quasi-steady flutter speed is just 40% of the unsteady flutter speed. These results thus differ the most of all the examples

presented. Nevertheless, the unsteady flutter speed calculation is within 2% of that published in NACA TR 685 (Reference 14) of 492.7 knots.

#### 4.2.4.6 CG Variation Survey

This section shows a markedly lower slope for the flutter speed variation curve. This indicates a reduced sensitivity to CG shift due to the high torsional stiffness. The quasi-steady and unsteady flutter speeds are seen to agree at the CG position of about 0.7c.



4.2.5 Example Five: Example from USAAF Technical Report 4798,  
(Smilg, Wasserman, 1942)

4.2.5.1 Inputs, Intermediate Calculations and Outputs

**Program Inputs**

Section Chord	132	Inch
Strip Width	10	Inch
AC location	0.25	Tenths of chord
CG Location	0.39	Tenths of chord
EA Location	0.31	Tenths of chord
Section Bending Stiffness	114	Pounds per Inch
Section Torsional Stiffness	279963	Inch-Pounds per Radian
Section Weight per unit span	8.5	Pounds per Inch
Section Mass Moment of Inertia about CG	198	Slug-inch <sup>2</sup> per inch
Air Density at ISA conditions	0.00237	Slugs/cubic foot
	8	
Test Altitude	10000	Feet
Airfoil Lift Curve Slope	0.109	Per degree

**Intermediate Calculations**

Air Density Ratio at Test Condition	0.7383	Non Dimensional
Uncoupled Natural Bending Frequency	20.78	Radians/Sec
Uncoupled Natural Torsional Frequency	35.08	Radians/Sec
CG Position	0.16	Non Dimensional
EA Position	-0.38	Non Dimensional
Section Static Imbalance	2.788	Slug-inch

Radius of Gyration	0.4447	Non Dimensional
Mass ratio	18.98	Non Dimensional
Static Divergence Speed	453.9	Knots

**Program Outputs**

Quasi-steady (QS) Flutter Frequency	33.5	Radians/Sec
Quasi-steady (QS) Flutter Speed	135.0	Knots
Reduced Frequency (k) at Zero Damping	0.4	Non Dimensional
Unsteady (US) Flutter Frequency	27.08	Radians/Sec
Unsteady (US) Flutter Speed	220.7	Knots
Ratio of QS to US flutter frequency	1.24	Non Dimensional
Ratio of QS to US flutter speed	0.61	Non Dimensional

4.2.5.2 Section Characteristics

This section appeared to be taken from an all-aluminum, semi-monocoque construction multi-engine transport or bomber aircraft.

This section has the highest mass ratio of the series, suggesting greater flutter resistance. The section is also the most massive of the series sections, probably due to contribution of the wing mounted engine in the section weight. Test altitude was 10,000 feet. No published results for the bending-torsion flutter frequency or speed for this airfoil section

were available in Technical Report 4798.

#### 4.2.5.3 Flutter Calculations for the Quasi-steady Case

The flutter frequency of 33.5 rad/sec is between the bending and torsional natural frequencies. The flutter speed is calculated at 135 knots.

#### 4.2.5.4 Flutter Calculations for the Unsteady Case

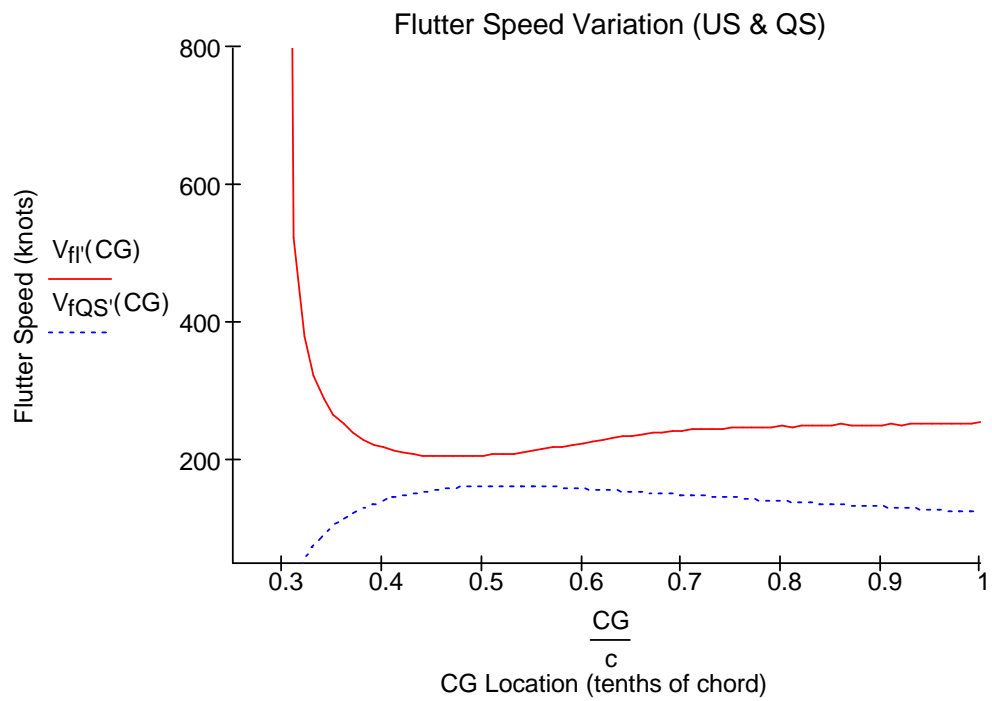
The reduced frequency at zero artificial damping is 0.4. The unsteady flutter frequency is between both the natural bending and torsional frequencies, coming in at 27.08 rad/sec. This section had the lowest coupled flutter frequency of the series. The flutter speed is 220.7 knots.

#### 4.2.5.5 Comparison of Results in the Quasi-steady and Unsteady Cases

The quasi-steady flutter frequency is 124% of the unsteady flutter frequency, while the quasi-steady flutter speed is 61% of the unsteady flutter speed. This continues the typical trend of results for the quasi-steady case of about 60% of the calculated critical flutter speed when compared to the unsteady case.

#### 4.2.5.6 CG Variation Survey

The section shows profound sensitivity to CG location. The high mass of the section seems to predominate among the three forces as far as sensitivity to flutter speed change.



4.2.6 Example Six: Example from Reference 5, page 203 (Scanlan, Rosenbaum, 1968)

4.2.6.1 Inputs, Intermediate Calculations and Outputs

**Program Inputs**

Section Chord	75	Inch
Strip Width	10	Inch
AC location	0.25	Tenths of chord
CG Location	0.46	Tenths of chord
EA Location	0.35	Tenths of chord
Section Bending Stiffness	210	Pounds per Inch
Section Torsional Stiffness	409875	Inch-Pounds per Radian
Section Weight per unit span	1.75	Pounds per Inch
Section Mass Moment of Inertia about CG	36.7	Slug-inch <sup>2</sup> per inch
Air Density at ISA conditions	0.002378	Slugs/cubic foot
Test Altitude	20000	Feet
Airfoil Lift Curve Slope	0.104	Per degree

**Intermediate Calculations**

Air Density Ratio at Test Condition	0.5326	Non Dimensional
Uncoupled Natural Bending Frequency	62.16	Radians/Sec
Uncoupled Natural Torsional Frequency	100.73	Radians/Sec
CG Position	0.22	Non Dimensional
EA Position	-0.3	Non Dimensional
Section Static Imbalance	0.488	Slug-inch
Radius of Gyration	0.727	Non Dimensional
Mass ratio	16.79	Non Dimensional
Static Divergence Speed	902.4	Knots

### **Program Outputs**

Quasi-steady (QS) Flutter Frequency	96.78	Radians/Sec
Quasi-steady (QS) Flutter Speed	250.2	Knots
Reduced Frequency (k) at Zero Damping	0.4	Non Dimensional
Unsteady (US) Flutter Frequency	89.29	Radians/Sec
Unsteady (US) Flutter Speed	384.7	Knots
Ratio of QS to US flutter frequency	1.08	Non Dimensional
Ratio of QS to US flutter speed	0.65	Non Dimensional

#### 4.2.6.2 Section Characteristics

This section is taken from the textbook listed above. The aircraft type is unknown. Test altitude was 20,000 feet. The section has the highest natural torsional frequency of the six section tested.

#### 4.2.6.3 Flutter Calculations for the Quasi-steady Case

Flutter frequency is 96.78 rad/sec, falling between the bending and torsional natural frequencies. The flutter speed is 250.2 knots.

#### 4.2.6.4 Flutter Calculations for the Unsteady Case

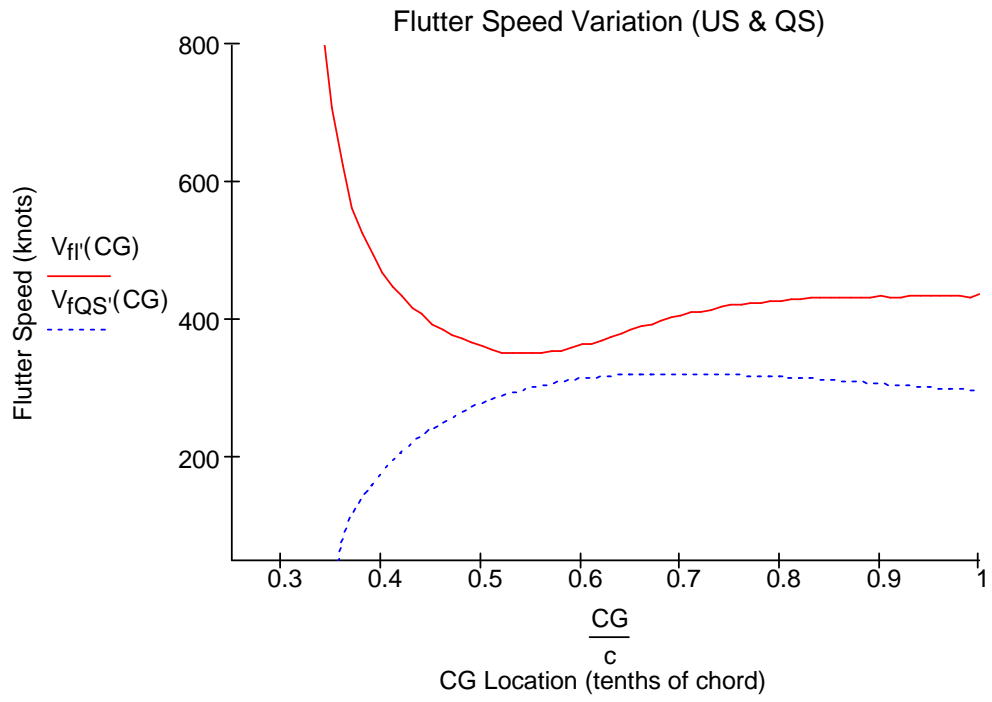
The reduced frequency for zero artificial damping in the unsteady case is 0.4. The flutter frequency is 89.29 Rad/sec, and the flutter speed is 384.7 knots. The flutter speed range is above the range of validity for incompressible flow. Further evaluation would be required to refine the flutter speeds determined here.

#### 4.2.6.5 Comparison of Results in the Quasi-steady and Unsteady Cases

The quasi-steady flutter frequency is 108 % of the unsteady flutter frequency, while the quasi-steady flutter speed is 61% of the unsteady flutter speed for the given conditions.

#### 4.2.6.6 CG Variation Survey

The high natural torsional frequency here seems to reduce the slope of the flutter speed variation curve. This section had the highest Divergence speed, the highest quasi-steady flutter frequency and the highest quasi-steady flutter speed of all the tested sections.



### 4.3 Chapter Summary

The attached spreadsheet summarizes the results of five test sections. Comparison of the quasi-steady to the unsteady flutter speeds typically shows the quasi-steady speeds to be about 60-65% of those when unsteady aerodynamic forces are used. In one case the quasi-steady flutter speed was only 40% of the unsteady flutter speed.

The results of the CG study were in agreement only when the value of the lever arm distance from the CG to the EA was about 0.25 in non-dimensional terms. For this range, the 60-70% trend found in the quasi-steady to unsteady flutter speeds is supported.

The Mathcad worksheet may be used to investigate potential solutions to unacceptably low flutter speeds. The results of trial calculations may then be reviewed by use of the worksheets to determine the most favorable method to change the flutter speed according to the design requirements and the options available to the designer.

Prevention or mitigation of flutter can be accomplished by adjustment of key structural and aerodynamic parameters, such as:

1. Section geometric properties, including section chord and airfoil section profile;
2. Structural properties, including the bending and the torsional stiffnesses and elastic axis location;
3. Inertial properties, including section mass, mass moment of inertia, and center of gravity position.
4. Aerodynamic properties for the desired test condition, i.e., Sea Level or at altitude.

Active flutter suppression measures, such as smart structures, can alter stiffness on demand, thereby altering the structural variables as required by operational conditions. This increases flutter speed while keeping weight growth in control. This approach has been investigated using a wind tunnel model in the Piezoelectric Aeroelastic Response Tailoring Investigation (PARTI) program cited in Reference 16.

**Table 4.3**

**Summary of Program Inputs, Calculations and Outputs**

	<b>Ryan NYP Proto- type (1)</b>	<b>MD3- 160 (3)</b>	<b>Ref 14, p. 108 (4)</b>	<b>Ref 11, p. 155 (5)</b>	<b>Ref 5, p. 203 (6)</b>	<b>Unit</b>
<b><u>Program Inputs</u></b>						
Section Chord	84	60	144	132	75	Inch
Strip Width	10	10	10	10	10	Inch
AC location	0.25	0.25	0.25	0.25	0.25	Tenths of chord
CG Location	0.4	0.5	0.4	0.39	0.46	Tenths of chord
EA Location	0.26	0.4	0.3	0.31	0.35	Tenths of chord
Section Bending Stiffness	12.25	114	45.4	114	210	Pounds /Inch
Section Torsional Stiffness	6084	132756	948572	279963	409875	Inch- Pounds /Radian
Section Weight per unit span	0.81	0.83	2.9	8.5	1.75	Pounds /Inch
Section Mass Moment of Inertia about CG	8.75	13.74	97.6	198	36.7	Slug- inch <sup>2</sup> per inch
Air Density at ISA conditions	0.0024	0.0024	0.0024	0.0024	0.0024	Slugs /cubic ft
Test Altitude	0	0	0	10000	20000	Feet
Airfoil Lift Curve Slope	0.084	0.104	0.104	0.109	0.104	Per degree

### **Intermediate Calculations**

Air Density Ratio at Test Condition	1.0	1.0	1.0	0.7383	0.5326	Non Dimens.
Uncoupled Natural Bending Frequency	22.1	66.5	22.45	20.78	62.16	Radians /Sec
Uncoupled Natural Torsional Frequency	22.3	95.14	90.32	35.08	100.73	Radians /Sec
CG Position	0.28	0.2	0.2	0.16	0.22	Non Dimens.
EA Position	-0.48	-0.2	-0.4	-0.38	-0.3	Non Dimens.
Section Static Imbalance	0.296	0.155	1.297	2.788	0.488	Slug-inch
Radius of Gyration	0.525	0.7952	0.499	0.4447	0.727	Non Dimens.
Mass ratio	3.3	6.62	4.02	18.98	16.79	Non Dimens.
Static Divergence Speed	252.1	382.5	737.9	453.9	902.4	Knots

### **Program Outputs**

#### **Quasi-steady Aerodynamics**

Quasi-steady (QS) Flutter Frequency	22.08	90.92	86.9	33.5	96.78	Radians /Sec
Quasi-steady (QS) Flutter Speed	35.6	112.6	201.2	135.0	250.2	Knots

## Unsteady Aerodynamics

Reduced Frequency (k) at Zero Damping	1.06	0.85	0.40	0.40	0.43	Non Dimens.
Phase Angle at Zero Damping	8.3	60.2	68.00	72.00	72.50	Degrees
Unsteady (US) Flutter Frequency	27.32	91.34	56.32	27.08	89.29	Radians/ Sec
Unsteady (US) Flutter Speed	53.5	159.3	500.8	220.7	384.7	Knots
Ratio of QS to US flutter frequency	0.81	1.00	1.54	1.24	1.08	Non Dimens.
Ratio of QS to US flutter speed	0.67	0.71	0.40	0.61	0.65	Non Dimens.

This Page Intentionally Left Blank

## Appendix

Sample Mathcad Bending-Torsion Flutter Worksheet.....	105
---	-----

This Page Intentionally Left Blank

## Bending-Torsion Flutter Worksheet

Airfoil Section Analyzed: From Scanlon & Rosenbaum,  
p. 203

### Program Inputs and Preliminary Calculations

#### Geometric Properties

##### Section Dimensions

Section Chord                      Strip width  
 $c = 75$  in                       $w = 10$  in

Location of section aerodynamic center  
(tenths of chord aft of leading edge)

$AC = 0.25c$      $AC = 18.75$  in

Location of section center of gravity  
(tenths of chord aft of leading edge)

$CG = 0.46c$      $CG = 34.5$  in

Location of section elastic axis  
(tenths of chord aft of leading edge)

$EA = 0.35c$      $EA = 26.25$  in

#### Elastic Properties

Section Bending Stiffness per unit span

$k_b = 210$                        $\frac{\text{lb}}{\text{in}^2}$

Section Torsional Stiffness per unit span

$K_T = 409875$                        $\frac{\text{lb}}{\text{rad}}$

## Inertial Properties

Section Weight per  
inch

$$\boxed{Wt = 1.75} \quad \text{lbf}$$

Section Mass Moment of Inertia about  
CG per inch span

$$\boxed{H_{cg} = 36.7} \quad \frac{\text{slug} \cdot \text{inch}^2}{\text{in}}$$

## Aerodynamic Properties

Air density at International Standard Atmosphere

$$\boxed{\rho_0 = 0.002378} \quad \frac{\text{slugs}}{\text{ft}^3}$$

Test Altitude

$$\boxed{Alt = 20000} \quad \text{feet}$$

Lift Curve Slope (no finite span corrections)

$$\boxed{C_{lx} = \frac{360}{2 \cdot \pi} \cdot 0.104} \quad C_{lx} = 5.96$$

---

## Supporting Calculations

Strip Area

$$S = w \cdot c \quad S = 750 \quad \text{in}^2$$

Section semi-chord

$$b' = \frac{c}{2} \quad \text{in} \quad b' = 37.5 \quad \text{in}$$

Distance from Section Elastic Axis to Section  
Aerodynamic Center (Positive forward of EA)

$$a = EA - AC \quad a = 7.5 \quad \text{in}$$

Distance from Section Elastic Axis to Section Center of Gravity (Negative aft of EA)

$$b = EA - CG \qquad b = -8.25 \quad \text{in}$$

Section Mass per inch

$$m = \frac{Wt}{32.2} \qquad m = 0.05435 \quad \frac{\text{slug}}{\text{in}}$$

Section mass moment of Inertia about Elastic Axis per inch

$$H_{ea} = H_{cg} + m \cdot b^2 \qquad H_{ea} = 40.4 \quad \frac{\text{slug} \cdot \text{inch}^2}{\text{in}}$$

Air Density ratio

$$\delta_{\infty} = (1 - 0.00000688 \cdot \text{Alt})^{4.256} \qquad \delta = 0.5326$$

Air density at test condition

$$\rho = \frac{\rho_0 \cdot \delta}{12^3} \qquad \rho = 7.33 \times 10^{-7} \quad \frac{\text{slugs}}{\text{in}^3}$$

Aerodynamic Lift Factor

$$A_0 = \frac{1}{2} \cdot \rho \cdot S \cdot C_{L\alpha} \quad \frac{\text{slug} \cdot \text{in}}{\text{rad}} \qquad A_0 = 1.64 \times 10^{-3} \quad \frac{\text{slug} \cdot \text{in}}{\text{rad}}$$

Strip Properties for Quasi-Steady Calculation

Strip Bending Stiffness

$$k_{b\text{strip}} = k_b \cdot w \qquad k_{b\text{strip}} = 2100 \quad \text{lbf}$$

Strip Torsional Stiffness

$$K_{T\text{strip}} = K_T \cdot w \qquad K_{T\text{strip}} = 4098750 \quad \frac{\text{lbf}}{\text{rad}}$$

Strip Weight

$$W_{T\text{strip}} = W_t \cdot w \qquad W_{T\text{strip}} = 17.5 \quad \text{lbf}$$

Strip Mass

$$m_{\text{strip}} = \frac{Wt_{\text{strip}}}{32.2} \qquad m_{\text{strip}} = 0.5435 \quad \text{slugs}$$

Strip Mass Moment of Inertia about CG

$$H_{\text{cgstrip}} = H_{\text{cg}} \cdot w \qquad H_{\text{cgstrip}} = 367 \quad \text{slug} \cdot \text{inch}^2$$

Strip mass moment of Inertia about Elastic Axis

$$H_{\text{eastrip}} = H_{\text{cgstrip}} + m_{\text{strip}} \cdot b^2 \qquad H_{\text{eastrip}} = 403.99 \quad \text{slug} \cdot \text{inch}^2$$

Uncoupled Natural Bending Frequency

$$\omega_b = \sqrt{\frac{k_b}{m}} \qquad \omega_b = 62.16 \quad \frac{\text{rad}}{\text{sec}}$$

$$f_b = \frac{\omega_b}{2 \cdot \pi} \qquad f_b = 9.89 \quad \text{Hz}$$

Uncoupled Natural Torsional Frequency

$$\omega_T = \sqrt{\frac{K_T}{H_{\text{ea}}}} \qquad \omega_T = 100.73 \quad \frac{\text{rad}}{\text{sec}}$$

$$f_T = \frac{\omega_T}{2 \cdot \pi} \qquad f_T = 16.03 \quad \text{Hz}$$

Uncoupled Natural Bending-Torsion Frequency Ratios

$$\frac{\omega_b}{\omega_T} = 0.62 \qquad \frac{\omega_T}{\omega_b} = 1.62$$

$$\left(\frac{\omega_b}{\omega_T}\right)^2 = 0.38 \qquad \left(\frac{\omega_T}{\omega_b}\right)^2 = 2.63$$

Dimensionless CG position  
(Positive aft of EA):

$$x_{\alpha} = \frac{-b}{b'} \qquad x_{\alpha} = 0.22$$

Dimensionless EA position  
(Positive aft of midchord):

$$a_h = \frac{EA - b'}{b'}$$

$$a_h = -0.3$$

Section Static Imbalance per inch span

$$S_{\alpha} = m \cdot b' \cdot x_{\alpha}$$

$$S_{\alpha} = 0.448 \quad \text{slug} \cdot \text{in}$$

Dimensionless Radius of Gyration

$$r_{\alpha} = \sqrt{\frac{H_{ea}}{m \cdot b'^2}}$$

$$r_{\alpha} = 0.727$$

$$r_{\alpha}^2 = 0.5286$$

Mass ratio

$$\mu = \frac{m}{\pi \rho \cdot b'^2}$$

$$\mu = 16.79$$

Check of Airfoil Static Divergence  
Airspeed

$$V_D = \sqrt{\frac{2 \cdot K_{Tstrip}}{a \cdot S \cdot \rho \cdot C_{I\alpha}}}$$

$$V_D = 18267.5 \quad \frac{\text{in}}{\text{sec}}$$

$$\frac{V_D}{12} = 1522.29 \quad \frac{\text{ft}}{\text{sec}}$$

$$0.0494V_D = 902.41 \quad \text{knots}$$

## Quasi-Steady Calculations

### Quasi-Steady Flutter Frequency

$$\omega_{fQS} = \sqrt{\frac{K_{Tstrip}}{H_{eastrip} - m_{strip} \cdot a \cdot b}} \quad \omega_{fQS} = 96.78 \quad \frac{\text{Rad}}{\text{sec}}$$

$$f_{fQS} = \frac{\omega_{fQS}}{2 \cdot \pi} \quad \boxed{f_{fQS} = 15.4} \quad \text{Hz}$$

### Quasi-Steady Flutter Speed

$$V_{fQS} = \sqrt{\frac{\left[ \left( k_{bstrip} - m_{strip} \cdot \omega_{fQS}^2 \right) \cdot \left( K_{Tstrip} - H_{eastrip} \cdot \omega_{fQS}^2 \right) \dots \right.}{\left. + \left( m_{strip} \cdot b \cdot \omega_{fQS}^2 \right)^2 \right]}{A_0 \cdot \left[ a \cdot \left( k_{bstrip} - m_{strip} \cdot \omega_{fQS}^2 \right) + b \cdot \left( m_{strip} \cdot \omega_{fQS}^2 \right) \right]}}$$

$$V_{fQS} = 5063.84 \quad \frac{\text{in}}{\text{sec}}$$

$$\frac{V_{fQS}}{12} = 421.99 \quad \frac{\text{ft}}{\text{sec}}$$

$$\boxed{0.0494 V_{fQS} = 250.2} \quad \text{knots}$$

### Quasi-Steady Flutter Frequency Ratio

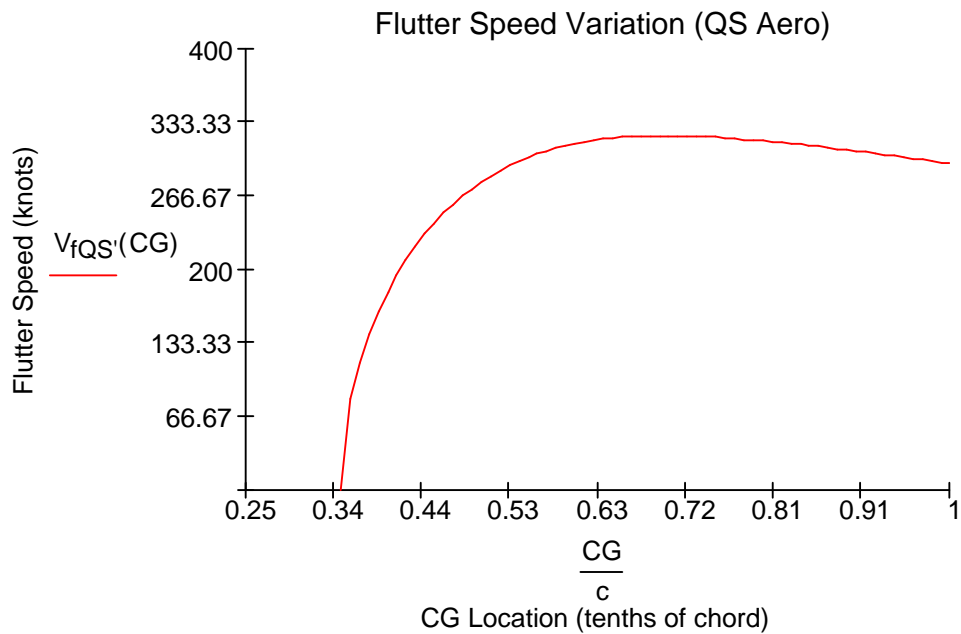
$$\frac{\omega_T}{\omega_{fQS}} = 1.04$$

$$\frac{\omega_{fQS}}{\omega_T} = 0.96$$

## Flutter Speed Variation with CG Shift using Quasi-Steady Aerodynamics

$$\text{CG} = 0.25c, 0.26c, \dots, c$$

$$V_{fQS}(CG) = \begin{cases} b \leftarrow EA - CG \\ H_{easstrip} \leftarrow H_{cgstrip} + m_{strip} \cdot b^2 \\ \omega_{fQS} \leftarrow \sqrt{\frac{K_{Tstrip}}{H_{easstrip} - m_{strip} \cdot a \cdot b}} \\ V_{fQS} \leftarrow \sqrt{\frac{(k_{bstrip} - m_{strip} \cdot \omega_{fQS}^2) \cdot (K_{Tstrip} - H_{easstrip} \cdot \omega_{fQS}^2) + -(m_{strip} \cdot b \cdot \omega_{fQS}^2)^2}{A_0 \cdot \left[ a \cdot (k_{bstrip} - m_{strip} \cdot \omega_{fQS}^2) \dots + b \cdot (m_{strip} \cdot \omega_{fQS}^2) \right]}} \\ V_{fQS} \leftarrow 0.0494 \cdot V_{fQS} \end{cases}$$



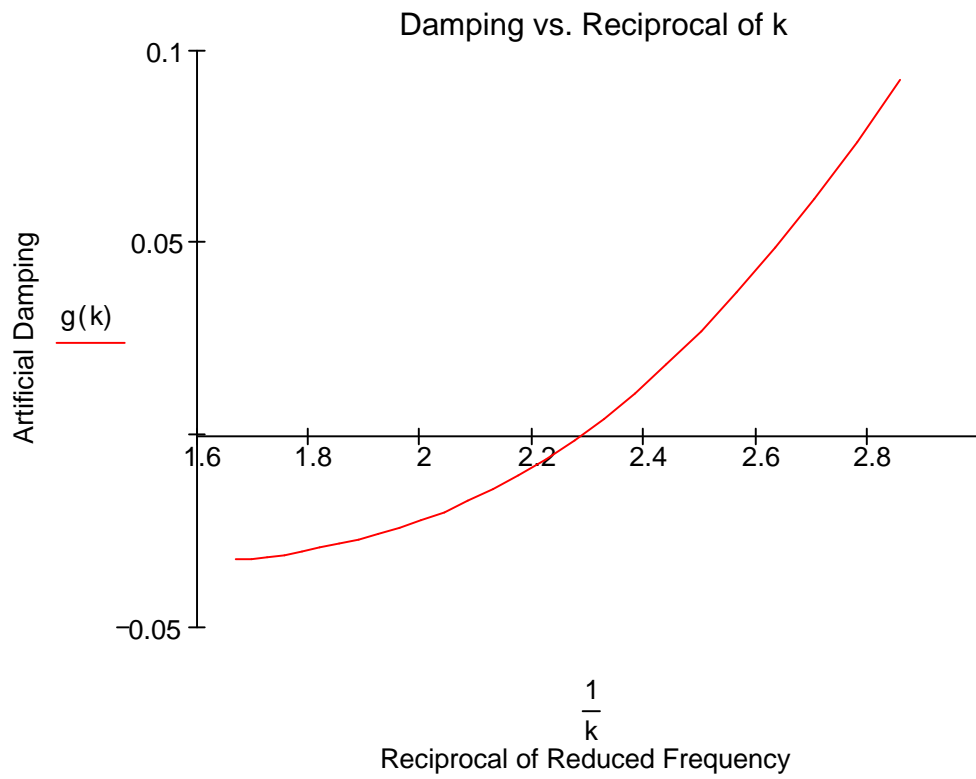
## Unsteady Calculations

Artificial Damping vs. Reciprocal of Reduced Frequency

$$k = 0.6, 0.59 \dots 0.35$$

$$g(k) = \left[ \begin{array}{l} F \leftarrow \frac{J1(k) \cdot (J1(k) + Y0(k)) + Y1(k) \cdot (Y1(k) - J0(k))}{(J1(k) + Y0(k))^2 + (Y1(k) - J0(k))^2} \\ G \leftarrow \frac{-Y1(k) \cdot Y0(k) - J1(k) \cdot J0(k)}{(J1(k) + Y0(k))^2 + (Y1(k) - J0(k))^2} \\ C \leftarrow F + i \cdot G \\ L_h \leftarrow 1 - 2 \cdot i \cdot \left(\frac{1}{k}\right) \cdot C \\ L_\alpha \leftarrow 0.5 - i \cdot \left(\frac{1}{k}\right) \cdot (1 + 2 \cdot C) - 2 \cdot \left(\frac{1}{k}\right)^2 \cdot C \\ M_h \leftarrow 0.5 \\ M_\alpha \leftarrow 0.375 - i \cdot \left(\frac{1}{k}\right) \\ A \leftarrow \left[ \begin{array}{ccc} \mu + \text{Re}(L_h) & i \cdot (\text{Im}(L_h)) & -\mu \cdot \left(\frac{\omega_b}{\omega_T}\right)^2 \end{array} \right]^T \\ B \leftarrow \mu \cdot x_\alpha + L_\alpha - L_h \cdot (0.5 + a_h) \\ D \leftarrow \mu \cdot x_\alpha + M_h - L_h \cdot (0.5 + a_h) \\ p' \leftarrow \mu \cdot r_\alpha^2 - 0.5 \cdot (0.5 + a_h) + \text{Re}(M_\alpha) - (0.5 + a_h) \cdot \text{Re}(L_\alpha) \dots \\ \quad + (0.5 + a_h)^2 \cdot \text{Re}(L_h) \\ q' \leftarrow i \cdot \left[ \text{Im}(M_\alpha) - (0.5 + a_h) \cdot \text{Im}(L_\alpha) + (0.5 + a_h)^2 \cdot \text{Im}(L_h) \right] \\ t' \leftarrow -\mu \cdot r_\alpha^2 \\ E \leftarrow (p' \quad q' \quad t')^T \\ c' \leftarrow A_1 \cdot E_1 + A_2 \cdot E_2 + A_1 \cdot E_2 + A_2 \cdot E_1 - (B \cdot D) \\ b'' \leftarrow A_1 \cdot E_3 + A_3 \cdot E_1 + (A_2 \cdot E_3 + A_3 \cdot E_2) \\ a'' \leftarrow A_3 \cdot E_3 \end{array} \right.$$

$$\begin{cases} v \leftarrow (c' \ b'' \ a'')^T \\ Z \leftarrow \text{polyroots}(v) \\ g \leftarrow \frac{\text{Im}(Z_1)}{\text{Re}(Z_1)} \end{cases}$$



### Artificial Damping vs. Airflow velocity

$$\underline{k} = 0.6, 0.59 \dots 0.35$$

$$Z(k) = \left[ \begin{array}{l} F \leftarrow \frac{J1(k) \cdot (J1(k) + Y0(k)) + Y1(k) \cdot (Y1(k) - J0(k))}{(J1(k) + Y0(k))^2 + (Y1(k) - J0(k))^2} \\ G \leftarrow \frac{-Y1(k) \cdot Y0(k) - J1(k) \cdot J0(k)}{(J1(k) + Y0(k))^2 + (Y1(k) - J0(k))^2} \\ C \leftarrow F + i \cdot G \\ L_h \leftarrow 1 - 2 \cdot i \cdot \left(\frac{1}{k}\right) \cdot C \\ L_\alpha \leftarrow 0.5 - i \cdot \left(\frac{1}{k}\right) \cdot (1 + 2 \cdot C) - 2 \cdot \left(\frac{1}{k}\right)^2 \cdot C \\ M_h \leftarrow 0.5 \\ M_\alpha \leftarrow 0.375 - i \cdot \left(\frac{1}{k}\right) \\ A \leftarrow \left[ \begin{array}{ccc} \mu + \operatorname{Re}(L_h) & i \cdot (\operatorname{Im}(L_h)) & -\mu \cdot \left(\frac{\omega_b}{\omega_T}\right)^2 \end{array} \right]^T \\ B \leftarrow \mu \cdot x_\alpha + L_\alpha - L_h \cdot (0.5 + a_h) \\ D \leftarrow \mu \cdot x_\alpha + M_h - L_h \cdot (0.5 + a_h) \\ p' \leftarrow \mu \cdot r_\alpha^2 - 0.5 \cdot (0.5 + a_h) + \operatorname{Re}(M_\alpha) - (0.5 + a_h) \cdot \operatorname{Re}(L_\alpha) \dots \\ \quad + (0.5 + a_h)^2 \cdot \operatorname{Re}(L_h) \\ q' \leftarrow i \cdot \left[ \operatorname{Im}(M_\alpha) - (0.5 + a_h) \cdot \operatorname{Im}(L_\alpha) + (0.5 + a_h)^2 \cdot \operatorname{Im}(L_h) \right] \\ r' \leftarrow -\mu \cdot r_\alpha^2 \\ E \leftarrow ((p' \quad q' \quad r'))^T \\ c' \leftarrow A_1 \cdot E_1 + A_2 \cdot E_2 + A_1 \cdot E_2 + A_2 \cdot E_1 - (B \cdot D) \\ b'' \leftarrow A_1 \cdot E_3 + A_3 \cdot E_1 + (A_2 \cdot E_3 + A_3 \cdot E_2) \\ a'' \leftarrow A_3 \cdot E_3 \\ v \leftarrow ((c' \quad b'' \quad a''))^T \\ Z \leftarrow \text{polyroots}(v) \end{array} \right.$$

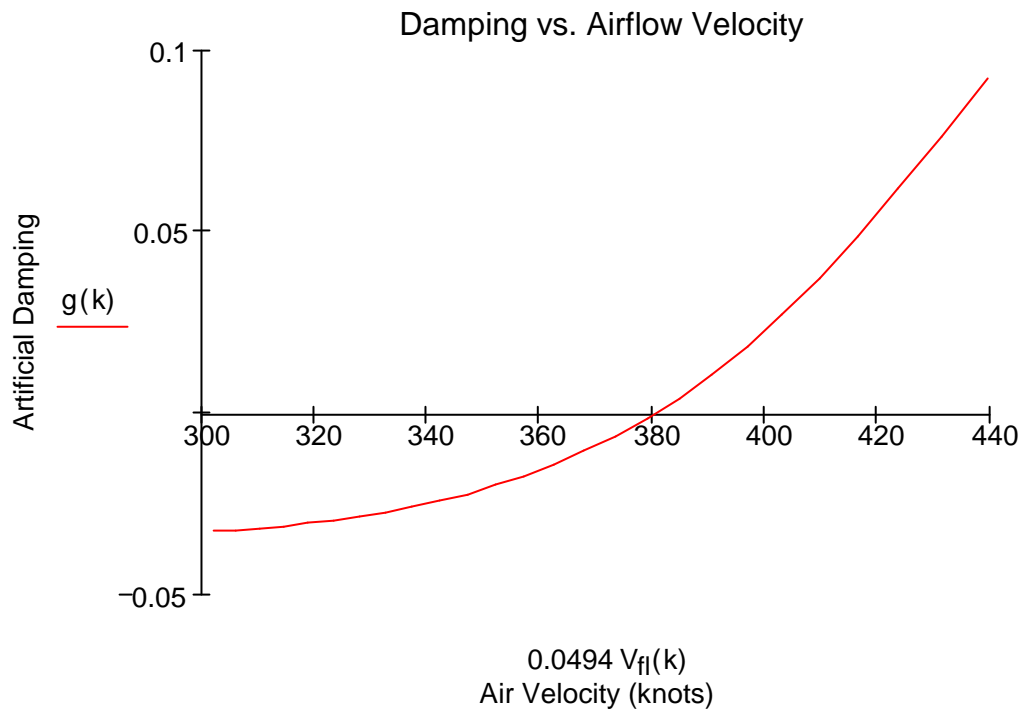
$$|Z_1| \leftarrow \text{Re}(Z_1)$$

Flutter Frequency (Radians/sec)

Flutter Speed (Inches/sec)

$$\omega_{fl}(k) = \frac{\omega_T}{\sqrt{Z(k)}}$$

$$V_{fl}(k) = \frac{\omega_{fl}(k) \cdot b'}{k}$$



## Unsteady Flutter Frequency and Speed Calculation

$$\begin{aligned}
 \underline{\omega} = & \left\{ \begin{array}{l}
 k \leftarrow 1.5 \\
 F \leftarrow \frac{J1(k) \cdot (J1(k) + Y0(k)) + Y1(k) \cdot (Y1(k) - J0(k))}{(J1(k) + Y0(k))^2 + (Y1(k) - J0(k))^2} \\
 G \leftarrow \frac{-Y1(k) \cdot Y0(k) - J1(k) \cdot J0(k)}{(J1(k) + Y0(k))^2 + (Y1(k) - J0(k))^2} \\
 C \leftarrow F + i \cdot G \\
 L_h \leftarrow 1 - 2 \cdot i \cdot \left(\frac{1}{k}\right) \cdot C \\
 L_\alpha \leftarrow 0.5 - i \cdot \left(\frac{1}{k}\right) \cdot (1 + 2 \cdot C) - 2 \cdot \left(\frac{1}{k}\right)^2 \cdot C \\
 M_h \leftarrow 0.5 \\
 M_\alpha \leftarrow 0.375 - i \cdot \left(\frac{1}{k}\right) \\
 A \leftarrow \left[ \begin{array}{ccc}
 \mu + \text{Re}(L_h) & i \cdot (\text{Im}(L_h)) & -\mu \cdot \left(\frac{\omega_b}{\omega_T}\right)^2
 \end{array} \right]^T \\
 B \leftarrow \mu \cdot x_\alpha + L_\alpha - L_h \cdot (0.5 + a_h) \\
 D \leftarrow \mu \cdot x_\alpha + M_h - L_h \cdot (0.5 + a_h) \\
 p' \leftarrow \mu \cdot r_\alpha^2 - 0.5 \cdot (0.5 + a_h) + \text{Re}(M_\alpha) - (0.5 + a_h) \cdot \text{Re}(L_\alpha) \dots \\
 \quad + (0.5 + a_h)^2 \cdot \text{Re}(L_h) \\
 q' \leftarrow i \cdot \left[ \text{Im}(M_\alpha) - (0.5 + a_h) \cdot \text{Im}(L_\alpha) + (0.5 + a_h)^2 \cdot \text{Im}(L_h) \right] \\
 t' \leftarrow -\mu \cdot r_\alpha^2 \\
 E \leftarrow ((p' \quad q' \quad t'))^T \\
 c' \leftarrow A_1 \cdot E_1 + A_2 \cdot E_2 + A_1 \cdot E_2 + A_2 \cdot E_1 - (B \cdot D) \\
 b'' \leftarrow A_1 \cdot E_3 + A_3 \cdot E_1 + (A_2 \cdot E_3 + A_3 \cdot E_2) \\
 a'' \leftarrow A_3 \cdot E_3 \\
 v \leftarrow ((c' \quad b'' \quad a''))^T
 \end{array} \right.
 \end{aligned}$$

```

Z ← polyroots(v)
g ←  $\frac{\text{Im}(Z_1)}{\text{Re}(Z_1)}$ 
while g < TOL
  k ← k - 0.01
  F ←  $\frac{J1(k) \cdot (J1(k) + Y0(k)) + Y1(k) \cdot (Y1(k) - J0(k))}{(J1(k) + Y0(k))^2 + (Y1(k) - J0(k))^2}$ 
  G ←  $\frac{-Y1(k) \cdot Y0(k) - J1(k) \cdot J0(k)}{(J1(k) + Y0(k))^2 + (Y1(k) - J0(k))^2}$ 
  C ← F + i · G
  Lh ←  $1 - 2 \cdot i \cdot \left(\frac{1}{k}\right) \cdot C$ 
  Lα ←  $0.5 - i \cdot \left(\frac{1}{k}\right) \cdot (1 + 2 \cdot C) - 2 \cdot \left(\frac{1}{k}\right)^2 \cdot C$ 
  Mh ← 0.5
  Mα ←  $0.375 - i \cdot \left(\frac{1}{k}\right)$ 
  A ←  $\left[ \begin{array}{ccc} \mu + \text{Re}(L_h) & i \cdot (\text{Im}(L_h)) & -\mu \cdot \left(\frac{\omega_b}{\omega_T}\right)^2 \end{array} \right]^T$ 
  B ←  $\mu \cdot x_\alpha + L_\alpha - L_h \cdot (0.5 + a_h)$ 
  D ←  $\mu \cdot x_\alpha + M_h - L_h \cdot (0.5 + a_h)$ 
  p' ←  $\mu \cdot r_\alpha^2 - 0.5 \cdot (0.5 + a_h) + \text{Re}(M_\alpha) - (0.5 + a_h) \cdot \text{Re}(L_\alpha) \dots$ 
   $+ (0.5 + a_h)^2 \cdot \text{Re}(L_h)$ 
  q' ←  $i \cdot \left[ \text{Im}(M_\alpha) - (0.5 + a_h) \cdot \text{Im}(L_\alpha) + (0.5 + a_h)^2 \cdot \text{Im}(L_h) \right]$ 
  t' ←  $-\mu \cdot r_\alpha^2$ 
  E ←  $((p' \quad q' \quad t'))^T$ 
  c' ←  $A_1 \cdot E_1 + A_2 \cdot E_2 + A_1 \cdot E_2 + A_2 \cdot E_1 - (B \cdot D)$ 
  b'' ←  $A_1 \cdot E_3 + A_3 \cdot E_1 + (A_2 \cdot E_3 + A_3 \cdot E_2)$ 
  a'' ←  $A_3 \cdot E_3$ 

```

$$\left| \begin{array}{l} v \leftarrow ((c' \ b'' \ a''))^T \\ Z \leftarrow \text{polyroots}(v) \\ g \leftarrow \frac{\text{Im}(Z_1)}{\text{Re}(Z_1)} \\ k \end{array} \right.$$

$$k = 0.43$$

$$F(k) = \frac{J1(k) \cdot (J1(k) + Y0(k)) + Y1(k) \cdot (Y1(k) - J0(k))}{(J1(k) + Y0(k))^2 + (Y1(k) - J0(k))^2}$$

$$G(k) = \frac{-Y1(k) \cdot Y0(k) - J1(k) \cdot J0(k)}{(J1(k) + Y0(k))^2 + (Y1(k) - J0(k))^2}$$

$$C(k) = F(k) + i \cdot G(k)$$

$$L_h(k) = 1 - 2 \cdot i \cdot \left(\frac{1}{k}\right) \cdot C(k)$$

$$L_\alpha(k) = 0.5 - i \cdot \left(\frac{1}{k}\right) \cdot (1 + 2 \cdot C(k)) - 2 \cdot \left(\frac{1}{k}\right)^2 \cdot C(k)$$

$$M_h = 0.5$$

$$M_\alpha(k) = 0.375 - i \cdot \left(\frac{1}{k}\right)$$

$$A = \left[ \begin{array}{cc} \mu + \text{Re}(L_h(k)) & i \cdot (\text{Im}(L_h(k))) \\ -\mu \cdot \left(\frac{\omega_b}{\omega_T}\right)^2 \end{array} \right]^T$$

$$B = \mu \cdot x_\alpha + L_\alpha(k) - L_h(k) \cdot (0.5 + a_h)$$

$$D = \mu \cdot x_\alpha + M_h - L_h(k) \cdot (0.5 + a_h)$$

$$p' = \mu \cdot r_\alpha^2 - 0.5 \cdot (0.5 + a_h) + \text{Re}(M_\alpha(k)) - (0.5 + a_h) \cdot \text{Re}(L_\alpha(k)) \dots \\ + (0.5 + a_h)^2 \cdot \text{Re}(L_h(k))$$

$$q' = i \cdot \left[ \text{Im}(M_\alpha(k)) - (0.5 + a_h) \cdot \text{Im}(L_\alpha(k)) + (0.5 + a_h)^2 \cdot \text{Im}(L_h(k)) \right]$$

$$t' = -\mu \cdot r_\alpha^2$$

$$E = (p' \quad q' \quad t')^T$$

$$c' = A_1 \cdot E_1 + A_2 \cdot E_2 + A_1 \cdot E_2 + A_2 \cdot E_1 - (B \cdot D)$$

$$b'' = A_1 \cdot E_3 + A_3 \cdot E_1 + A_2 \cdot E_3 + A_3 \cdot E_2$$

$$a'' = A_3 \cdot E_3$$

$$v(k) = (c' \quad b'' \quad a'')^T$$

$$\underline{\underline{Z}}(k) = \text{polyroots}(v(k))$$

### Artificial Damping

$$g = \frac{\text{Im}(Z(k)_1)}{\text{Re}(Z(k)_1)}$$

$$g = 0.0039$$

### Unsteady Flutter Frequency

$$\underline{\underline{\omega}}_{ff} = \frac{\omega_T}{\sqrt{\text{Re}(Z(k)_1)}}$$

$$\omega_{ff} = 89.29$$

$\frac{\text{Rad}}{\text{sec}}$

$$f_{ff} = \frac{\omega_{ff}}{2 \cdot \pi}$$

$$f_{ff} = 14.2$$

Hz

### Unsteady Flutter Speed

$$\underline{\underline{V}}_{ff} = \frac{\omega_{ff} \cdot b'}{k}$$

$$V_{ff} = 7787.28$$

$\frac{\text{in}}{\text{sec}}$

$$0.0494 V_{ff} = 384.7$$

knots

### Non-dimensional Flutter Speed

$$V_{flIND} = \frac{V_{fl}}{b' \cdot \omega_T}$$

$$V_{flIND} = 2.06$$

### Phase Angle

$$X = \left( \frac{\omega_T}{\omega_{fl}} \right)^2$$

$$A' = \mu \cdot \left[ 1 - Z(k) \cdot \left( \frac{\omega_b}{\omega_T} \right)^2 \cdot (1 + i \cdot g) \right] \cdot L_h(k)$$

$$E' = \mu \cdot r_{\alpha}^2 \cdot [1 - X \cdot (1 + i \cdot g)] - \frac{1}{2} \cdot \left( \frac{1}{2} + a_h \right) \dots$$

$$+ M_{\alpha}(k) - L_{\alpha}(k) \cdot \left( \frac{1}{2} + a_h \right) + L_h(k) \cdot \left( \frac{1}{2} + a_h \right)^2$$

$$\begin{pmatrix} A' & B \\ D & E' \end{pmatrix} = \begin{pmatrix} 2.01 - 24.79i & -3.27 - 2.88i \\ 4.14 + 0.57i & -0.75 - 1.79i \end{pmatrix}$$

$$\text{Phase} = (A' \ B) - \frac{B}{E'} \cdot (D \ E')$$

$$\text{Phase} = (-6.9 - 21.9i \ 0)$$

$$\phi = 180 + \arg(\min(\text{Phase})) \cdot \frac{360}{2 \cdot \pi}$$

$$\phi = 72.5 \quad \text{deg}$$

### Comparison of Quasi-steady and Unsteady results:

Quasi-Steady flutter frequency and speed:

$$f_{QS} = 15.4 \quad \text{Hz}$$

$$0.0494 V_{fQS} = 250.2 \quad \text{knots}$$

Unsteady flutter frequency and speed:

$$f_{fl} = 14.21 \quad \text{Hz}$$

$$0.0494 V_{fl} = 384.7 \quad \text{knots}$$

$$\frac{f_{QS}}{f_{fl}} = 1.08$$

$$\frac{V_{fQS}}{V_{fl}} = 0.65$$

## Flutter Speed Variation with CG Shift Using Unsteady Aerodynamics

$$\text{CG} = 0.25c, 0.26c \dots c$$

$$V_{fl}(CG) = \left[ \begin{array}{l} k \leftarrow 3.0 \\ b \leftarrow EA - CG \\ H_{ea} \leftarrow H_{cg} + m \cdot b^2 \\ r_{\alpha} \leftarrow \sqrt{\frac{H_{ea}}{m \cdot b'^2}} \\ x_{\alpha} \leftarrow \frac{-b}{b'} \\ \omega_T \leftarrow \sqrt{\frac{K_T}{H_{ea}}} \\ F \leftarrow \frac{J1(k) \cdot (J1(k) + Y0(k)) + Y1(k) \cdot (Y1(k) - J0(k))}{(J1(k) + Y0(k))^2 + (Y1(k) - J0(k))^2} \\ G \leftarrow \frac{-Y1(k) \cdot Y0(k) - J1(k) \cdot J0(k)}{(J1(k) + Y0(k))^2 + (Y1(k) - J0(k))^2} \\ C \leftarrow F + i \cdot G \\ L_h \leftarrow 1 - 2 \cdot i \cdot \left(\frac{1}{k}\right) \cdot C \\ L_{\alpha} \leftarrow 0.5 - i \cdot \left(\frac{1}{k}\right) \cdot (1 + 2 \cdot C) - 2 \cdot \left(\frac{1}{k}\right)^2 \cdot C \\ M_h \leftarrow 0.5 \\ M_{\alpha} \leftarrow 0.375 - i \cdot \left(\frac{1}{k}\right) \\ A \leftarrow \left[ \begin{array}{ccc} \mu + \text{Re}(L_h) & i \cdot (\text{Im}(L_h)) & -\mu \cdot \left(\frac{\omega_b}{\omega_T}\right)^2 \end{array} \right]^T \\ B \leftarrow \mu \cdot x_{\alpha} + L_{\alpha} - L_h \cdot (0.5 + a_h) \\ D \leftarrow \mu \cdot x_{\alpha} + M_h - L_h \cdot (0.5 + a_h) \\ p' \leftarrow \mu \cdot r_{\alpha}^2 - 0.5 \cdot (0.5 + a_h) + \text{Re}(M_{\alpha}) - (0.5 + a_h) \cdot \text{Re}(L_{\alpha}) \dots \\ \quad + (0.5 + a_h)^2 \cdot \text{Re}(L_h) \end{array} \right.$$

```

q' ← i · [ Im(Mα) - (0.5 + ah) · Im(Lα) + (0.5 + ah)2 · Im(Lh) ]
t' ← -μ · rα2
E ← ((p' q' t'))T
c' ← A1 · E1 + A2 · E2 + A1 · E2 + A2 · E1 - (B · D)
b'' ← A1 · E3 + A3 · E1 + (A2 · E3 + A3 · E2)
a'' ← A3 · E3
v ← ((c' b'' a''))T
Z ← polyroots(v)
g ←  $\frac{\text{Im}(Z_1)}{\text{Re}(Z_1)}$ 
while g < TOL
    k ← k - 0.01
    F ←  $\frac{J_1(k) \cdot (J_1(k) + Y_0(k)) + Y_1(k) \cdot (Y_1(k) - J_0(k))}{(J_1(k) + Y_0(k))^2 + (Y_1(k) - J_0(k))^2}$ 
    G ←  $\frac{-Y_1(k) \cdot Y_0(k) - J_1(k) \cdot J_0(k)}{(J_1(k) + Y_0(k))^2 + (Y_1(k) - J_0(k))^2}$ 
    C ← F + i · G
    Lh ← 1 - 2 · i ·  $\left(\frac{1}{k}\right)$  · C
    Lα ← 0.5 - i ·  $\left(\frac{1}{k}\right)$  · (1 + 2 · C) - 2 ·  $\left(\frac{1}{k}\right)^2$  · C
    Mh ← 0.5
    Mα ← 0.375 - i ·  $\left(\frac{1}{k}\right)$ 
    A ←  $\left[ \begin{array}{ccc} \mu + \text{Re}(L_h) & i \cdot (\text{Im}(L_h)) & -\mu \cdot \left(\frac{\omega_b}{\omega_T}\right)^2 \end{array} \right]^T$ 
    B ← μ · xα + Lα - Lh · (0.5 + ah)
    D ← μ · xα + Mh - Lh · (0.5 + ah)

```

$$p' \leftarrow \mu \cdot r_{\alpha}^2 - 0.5 \cdot (0.5 + a_h) + \operatorname{Re}(M_{\alpha}) - (0.5 + a_h) \cdot \operatorname{Re}(L_{\alpha}) + (0.5 + a_h)^2 \cdot \operatorname{Re}(L_h)$$

$$q' \leftarrow i \cdot [\operatorname{Im}(M_{\alpha}) - (0.5 + a_h) \cdot \operatorname{Im}(L_{\alpha}) + (0.5 + a_h)^2 \cdot \operatorname{Im}(L_h)]$$

$$t' \leftarrow -\mu \cdot r_{\alpha}^2$$

$$E \leftarrow ((p' \quad q' \quad t'))^T$$

$$c' \leftarrow A_1 \cdot E_1 + A_2 \cdot E_2 + A_1 \cdot E_2 + A_2 \cdot E_1 - (B \cdot D)$$

$$b'' \leftarrow A_1 \cdot E_3 + A_3 \cdot E_1 + (A_2 \cdot E_3 + A_3 \cdot E_2)$$

$$a'' \leftarrow A_3 \cdot E_3$$

$$v \leftarrow ((c' \quad b'' \quad a''))^T$$

$$Z \leftarrow \text{polyroots}(v)$$

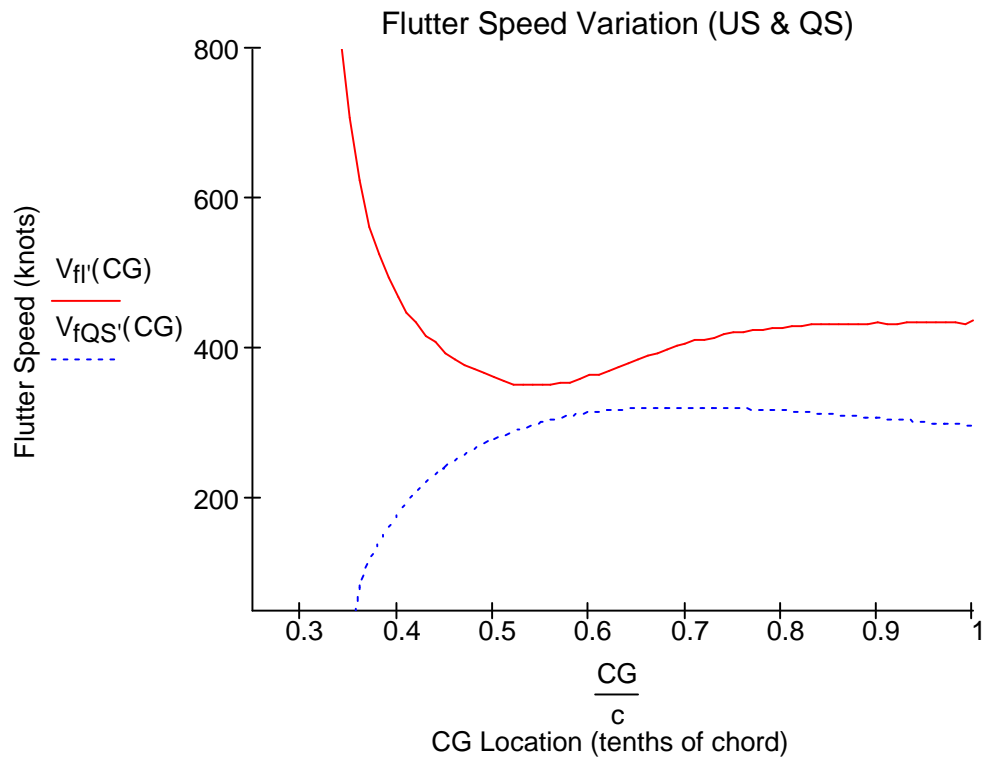
$$g \leftarrow \frac{\operatorname{Im}(Z_1)}{\operatorname{Re}(Z_1)}$$

k

$$\omega_{fl} \leftarrow \frac{\omega_T}{\sqrt{\operatorname{Re}(Z_1)}}$$

$$V_{fl} \leftarrow \frac{\omega_{fl} \cdot b'}{k}$$

$$0.0494V_{fl}$$



## References

1. Aeroelasticity, Bisplinghoff, R.L., Ashley, H., Halfman, R.L., Dover Publications, Inc., Mineola, NY, 1955
2. Principles of Aeroelasticity, Bisplinghoff, R.L., Ashley, H., Dover Publications, Inc., Mineola, NY, 1962
3. An Introduction to the Theory of Aeroelasticity, Y.C. Fung, Dover Publications, Inc., New York, NY, 1969
4. Dynamics of Structures, Hurty, W.C., Rubinstein, M.F., Prentice Hall, Inc., Englewood Cliffs, NJ, 1964
5. Introduction to the Study of Aircraft Vibration and Flutter, Scanlon, R.H., Rosenbaum, R., Dover Publications, Inc, New York, NY, 1968
6. Theoretical Aerodynamics, Milne-Thompson, L.M., C.B.E., Fourth Edition, Dover Publications, New York, NY, 1958.
7. Analysis of Aircraft Structures, An Introduction, Donaldson, B.K., McGraw-Hill, Inc., 1993
8. Aerodynamics of Wings and Bodies, Ashley, H., Landahl, M., Dover Publications, Inc., Mineola, NY, 1965
9. Flow-Induced Vibration, Blevins, R.D., Krieger Publishing Co., Malabar, FL, 1990
10. Airplane Performance, Stability and Control, Perkins, C.D., Hage, R.E., John Wiley and Sons, Inc., New York, NY, 1949

11. Air Corps Technical Report No. 4798, Application of Three-Dimensional Flutter Theory to Aircraft Structures (with Corrections for the Effects of Control Surface Aerodynamic Balance and Geared Tabs), Smilg, B., Wasserman, L., War Department, Air Corps Materiel Division, Dayton, OH, 1942
12. The Oscillating Wing with Aerodynamically Balanced Elevator, Kussner, H.G., Schwartz, L., NACA Technical Manual No. 991, 1940
13. NACA Technical Report No. 496, General Theory of Aerodynamic Instability and the Mechanism of Flutter, Theodorsen, T., Langley Memorial Aeronautical Laboratory, Langley Field, VA, 1934
14. NACA Technical Report No. 685, Mechanism of Flutter; A Theoretical and Experimental Investigation of the Flutter Problem, Theodorsen, T., Garrick, I.E., Langley Memorial Aeronautical Laboratory, Langley Field, VA, 1938
15. Dynamic Response of the MD3-160 Aircraft's Wing Model in Steady Flow, Usmani, M.A.W., Ho, T.C., Department of Aerospace Engineering, University Putra Malaysia, Malaysia, 2003
16. NASA Technical Memorandum 112852, Research and Applications in Aeroelasticity and Structural Dynamics at the NASA Langley Research Center, Abel, I., Langley Research Center, Hampton, VA, 1997
17. Article on aeroelasticity found on the Internet at <http://asdl.kaist.ac.kr/intro/ae1.htm>
18. NACA Technical Report No. 824, Summary of Airfoil Data, Abbott, I.H., von Doenhoff, A.E., Stivers, L.S., Langley Memorial Aeronautical Laboratory, Langley Field, VA, 1945

19. A Manual for Writers of Term Papers, Theses, and Dissertations,  
Turabian, Kate L., Sixth Edition, Revised by John Grossman and Alice  
Bennett, The University of Chicago Press, Chicago, 1996

This Page Intentionally Left Blank